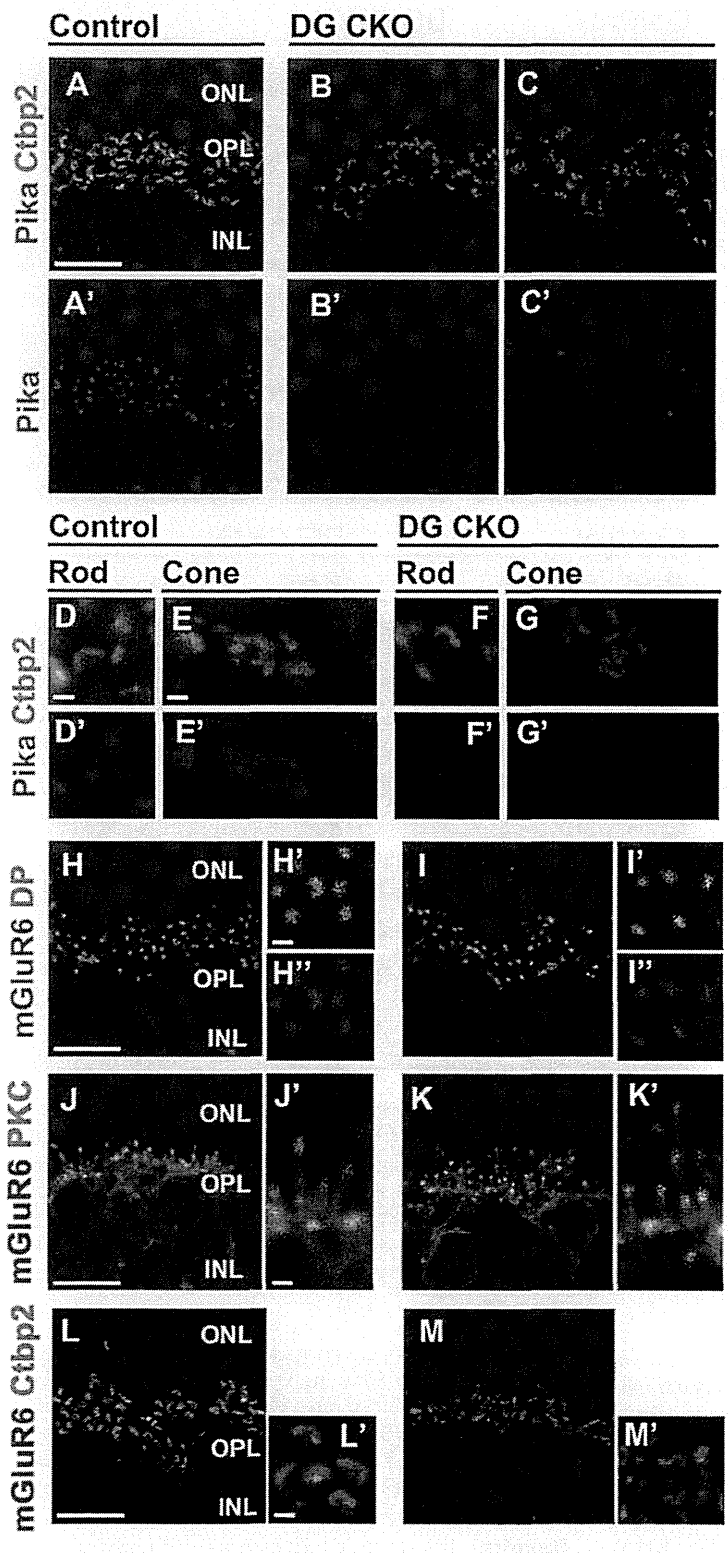

Figure 3. DG is essential for the proper localization of Pikachurin in the photoreceptor ribbon synapse. Immunostaining of photoreceptor synaptic markers in the *DG* CKO retina. Retinal sections from control (*A*, *A'*, *D*, *D'*, *E*, *E'*, *H–H''*, *J*, *J'*, *L*, *L'*) and *DG* CKO mice (*B*, *B'*, *C*, *C'*, *F*, *F'*, *G*, *G'*, *I–I''*, *K*, *K'*, *M*, *M'*) were stained with antibodies against Pikachurin (red in *A–G'*), CtBP2 (green in *A–G'*, *L–M'*), dystrophin (green in *H–I''*), PKC (green in *J–K'*; a marker for the dendrites of bipolar cells), mGluR6 (red in *H*, *H'*, *I*, *I'*, *J–M'*). Nuclei were stained with DAPI (blue). Higher-magnification views of rod (*D*, *D'*, *F*, *F'*) and cone (*E*, *E'*, *G*, *G'*) photoreceptor ribbon synapses were shown. Higher-magnification views of *H*, *I*, *J*, *K*, *L*, and *M* are shown in *H'*, *H''*, *I'*, *I''*, *J'*, *K'*, *L'*, and *M'*, respectively. In the control retina, Pikachurin signals were found in both rod and cone photoreceptor synapses, however, in the *DG* CKO retina, Pikachurin signals almost disappear. In contrast, the signals of dystrophin, mGluR6 and CtBP2 were undistinguishable between the control and *DG* CKO retinas. Scale bars: *A*, *H*, *J*, *L*, 10 μm; *D*, *E*, *H'*, *J'*, *L'*, 1 μm.

apposition of synaptic processes occurs, but synaptic processes have not invaginated into the photoreceptor axon terminals (Blanks et al., 1974). At this stage, we observed weak Pikachurin signals in the OPL adjacent to premature CtBP2-positive ribbons (Fig. 1*D*). DG and dystrophin signals were less intense than the Pikachurin signal at this stage; however, these signals were weakly concentrated at the OPL (Fig. 1*A*,*D*,*G*). Around P7–P10, horizontal cell synaptic processes invaginate into the photoreceptor terminal, whereas bipolar processes have not invaginated (Blanks et al., 1974). At P8, obvious DG and Pikachurin signal puncta were observed adjacent to the synaptic ribbon (Fig. 1*B*,*E*). Strong dystrophin signals were also detected in the OPL (Fig. 1*H*). This result suggests that Pikachurin, DG, and dystrophin were concentrated in the photoreceptor synaptic terminals before the invagination of bipolar processes. Around P10–P14, the invagination of bipolar processes occurs and photoreceptor synaptic maturation is almost complete (Blanks et al., 1974). At P12, photoreceptor synapses with DG and Pikachurin puncta in a horseshoe-like ribbon similar to those of the adult retina were found (Fig. 1*C*,*F*). At this stage, obvious dystrophin signal puncta were also observed in the OPL (Fig. 1*I*). These results suggest that photoreceptor DGC formation occurs between P8 and P12, just before the invagination of bipolar dendritic tips. To confirm the precise localization of DG and dystrophin in the OPL, we immunostained DG and dystrophin with a glutamate receptor, mGluR6, which localizes specifically in ON-bipolar dendritic tips. We observed that DG and dystrophin signals almost completely overlapped the mGluR6 signals at the photoreceptor synapses in the OPL (Fig. 1*J–K''*). In addition, the signals of another ON-bipolar dendritic tip marker, TRPM1, also overlapped the DG and dystrophin signals (Fig. 1*L–M''*). These results suggest that DG and dystrophin localize at the invagination of the bipolar dendritic terminus in the photoreceptor synaptic terminus.

Photoreceptor-specific DG defect affects the synaptic localization of Pikachurin

To investigate DG function in the photoreceptor ribbon synapse, we ablated DG from photoreceptor cells by conditional gene targeting. To accomplish this, we mated the $DG^{flox/flox}$ line (Moore et al., 2002) with the *Crx-Cre* transgenic mouse line in which Cre-mediated recombina-

tion occurs in both rod and cone photoreceptor precursors (Nishida et al., 2003). We generated $DG^{flox/flox}$;*Crx-Cre* (*DG* CKO) mice by mating $DG^{flox/flox}$ female mice with $DG^{flox/flox}$;*Crx-Cre* male mice. *DG* CKO mice were viable and fertile without apparent developmental abnormalities in the retina. To confirm the loss of DG in photoreceptors, retinal sections from adult control ($DG^{flox/flox}$) and *DG* CKO ($DG^{flox/flox}$;*Crx-Cre*) were stained with antibodies against β-DG and CtBP2 (Fig. 2*A–C′*). In the control retina, DG-positive puncta were observed in the OPL (Fig. 2*A,A′*). These DG signals were detected adjacent to horseshoe-like synaptic ribbons stained with CtBP2 (Fig. 2*A,A′*). In the *DG* CKO retina, although the CtBP2 signal was observed in the OPL, the DG signal was below detection level in most of the OPL (percentage of DG^+ $CtBP2^+$ synapses in $CtBP2^+$ synapses, 97.1 ± 1.9% in control, $n = 170$ from three animals, 10.7 ± 4.4% in *DG* CKO, $n = 137$ from three animals; $p < 0.01$) (Fig. 2*B–C′*). We observed a few DG-positive synapses remaining in the OPL (Fig. 2*C,C′*). In the mouse retina, ~97% of the photoreceptors were rod photoreceptors (Carter-Dawson and LaVail, 1979). A rod photoreceptor synaptic terminus contains a single ribbon (Fig. 2*D,F*), whereas a cone photoreceptor synapse contains a cluster of multiple ribbons (Fig. 2*E,G*). In the control retina, DG puncta were observed adjacent to both rod single ribbons (Fig. 2*D,D′*) and cone ribbon clusters (Fig. 2*E,E′*). In the *DG* CKO retina, no significant DG signal was observed adjacent to the rod single ribbon (Fig. 2*F,F′*) or cone ribbon clusters (Fig. 2*G,G′*).

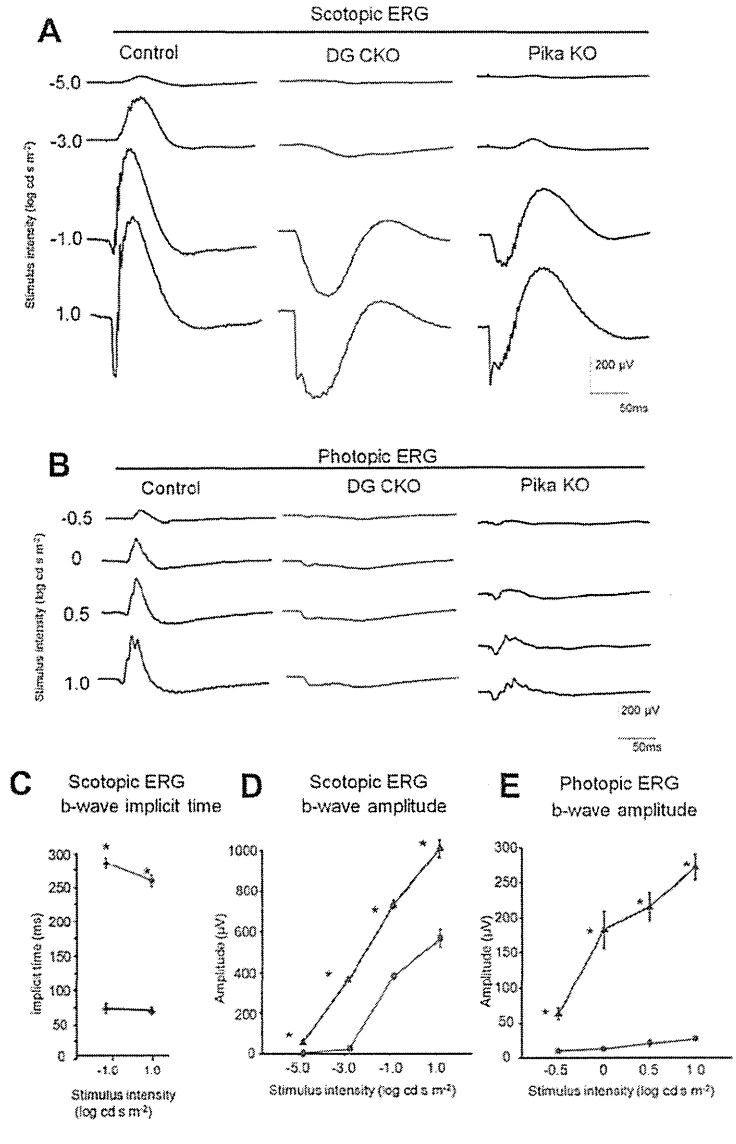

Figure 4. Electroretinograms recorded from *DG* CKO mice. Scotopic (*A*) and photopic (*B*) ERGs of an adult control mouse (left), a *DG* CKO mouse (middle) and *Pikachurin* KO mouse (right) are shown. Implicit time and amplitude of scotopic ERG b-waves as a function of the stimulus intensity are shown in *C* and *D* respectively. Amplitude of photopic ERG b-waves are shown in *E*. Blue lines indicate control ($n = 3$) and red lines indicate *DG* CKO ($n = 6$). *DG* CKO mice showed decreased amplitude under both scotopic and photopic conditions and prolongation of b-wave under scotopic conditions. The error bars indicate SEM. Asterisks indicate that the differences are statistically significant (Mann–Whitney test, $p < 0.05$).

In the normal retina, DG is also observed in the Müller glial endfeet abutting the ILM (Fig. 2*H,H′* arrowheads) and perivascular glial endfeet (Fig. 2*H*, arrows) (Schmitz and Drenckhahn, 1997b; Ueda et al., 2000; Blank et al., 2002). In contrast to the severe loss of DG in the OPL, DG signals remain in blood vessels (Fig. 2*I*, arrows) and the ILM (Fig. 2*I,I′* arrowheads) in the *DG* CKO retina. These results show that the loss of DG occurs specifically in rod and cone photoreceptors in the *DG* CKO retina.

Previous biochemical analysis showed that DG physically interacts with Pikachurin (Sato et al., 2008; Kanagawa et al., 2010). To examine whether the DG loss affects Pikachurin localization in photoreceptor synapses, we stained Pikachurin in adult control and *DG* CKO retinas. In the control retina, Pikachurin specifically localizes to the OPL in a punctate pattern adjacent to the synaptic ribbon stained with the anti-CtBP2 antibody in both rod and cone photoreceptor synapses (Fig. 3*A,D,E*). In contrast, the *DG* CKO retina showed an obvious loss of the Pikachurin signal in most of the OPL (percentage of $Pikachurin^+$ $CtBP2^+$ synapses in $CtBP2^+$ synapses, 97.7 ± 1.9% in control, $n = 204$ from four animals, 7.5 ± 4.8% in *DG* CKO, $n = 143$ from four animals; $p < 0.01$) (Fig. 3*B–C′,F–G′*), although a few Pikachurin puncta remain in the OPL (Fig. 3*C,C′*) as was observed with the DG signals (Fig. 2*C,C′*). The absence of the Pikachurin signal is observed in both rod and cone photoreceptor synaptic terminals (Fig. 3*F–G′*). This result suggests that DG in photoreceptors is essential for the synaptic localization of Pikachurin in photoreceptors. To investigate whether the deficiency of DG affects the integrity of bipolar dendritic structure, we performed immunostaining for mGluR6 and PKC, a marker for the ON-bipolar dendritic process. We found that mGluR6 signals accumulated at the tips of PKC-positive bipolar dendritic processes in both the control and *DG* CKO retinas (Fig. 3*J–K′*). In the normal retina, bipolar dendritic tips stained with mGluR6 localized adjacent to ribbons stained with CtBP2 (Fig. 3*L,L′*). Similarly, we found that the mGluR6 signal was observed adjacent to synaptic ribbons in

the *DG* CKO retina (percentage of mGluR6$^+$ CtBP2$^+$ synapses in CtBP2$^+$ synapses, 96.4 ± 1.6% in control, $n = 143$ from three animals, 92.1 ± 9.7% in *DG* CKO, $n = 65$ from three animals; $p > 0.05$) (Fig. 3*M*,*M*′). These results suggest that a deficiency of DG does not affect the gross structure of bipolar dendritic tips. DG directly interacts with dystrophin and forms the DGC in photoreceptor synapses. We next examined whether the loss of DG affects the distribution of dystrophin in the OPL. We observed the dystrophin signal colocalizing with mGluR6 in the OPL of control mice (Fig. 3*H*–*H*″). Unexpectedly, we observed a similar distribution of dystrophin in the *DG* CKO retina (percentage of dystrophin$^+$ mGluR6$^+$ puncta in mGluR6$^+$ puncta, 100% in control, $n = 191$ from four animals, 100% in *DG* CKO, $n = 207$ from four animals) (Fig. 3*I*–*I*″). Since dystrophin also interacts with the other DGC components and actin cytoskeleton, these interactions may be enough to keep dystrophin in the photoreceptor synaptic terminal without DG.

Loss of DG in photoreceptors affects synaptic signal transmission between photoreceptor and bipolar cells

Loss of Pikachurin causes the attenuation of ERG activity, and a reduced and prolonged b-wave in both scotopic and photopic conditions (Sato et al., 2008). Physical interaction between DG and Pikachurin *in vitro* suggests that DG plays an essential role in establishing a physiological connection between the photoreceptor terminus and bipolar dendrites (Sato et al., 2008; Kanagawa et al., 2010). To evaluate the physiological role of DG in the retina, we measured ERGs of adult *DG* CKO mice. We observed that *DG* CKO mice showed a decreased amplitude and prolonged b-wave under scotopic conditions (Fig. 4*A*,*C*,*D*). We found a decreased b-wave amplitude under photopic conditions (Fig. 4*B*,*E*). The ERG b-wave responses are mainly generated by the activity of ON-bipolar cells (Robson and Frishman, 1995, 1996; Koike et al., 2010). These results suggest an essential function of DG in the physiological connection between photoreceptors and ON-bipolar cells at ribbon synapses. Furthermore, we compared the degree of abnormality in ERGs between *DG* CKO and *Pikachurin* KO mice (Sato et al., 2008). Notably, the prolongation of b-wave implicit time under scotopic conditions was significantly more in the *DG* CKO mouse than in the *Pikachurin* KO mouse (Fig. 4*A*) (Sato et al., 2008). In addition, the b-wave amplitude under both photopic and scotopic conditions is less in the *DG* CKO mouse than in the *Pikachurin* KO mouse. These results indicate that loss of DG causes a more severe defect of synaptic connection between photoreceptor and bipolar cells than that caused by the loss of Pikachurin only.

Electron microscopic analysis of photoreceptor ribbon synapses in the *DG* CKO mice

To examine whether the loss of DG affects the ultrastructure of photoreceptor synapses, we performed 3D electron microscopic analyses on the adult control and *DG* CKO retinas. In this approach, projection images of longitudinal sections of photoreceptors were collected by tilting the specimen incrementally around an axis perpendicular to the electron beam. Using IMOD software, tomographic volumes (2.5 × 2.5 × 0.5 μm) of the rod synaptic terminus that included a large portion of the synapse ribbon were calculated from the series of projection images. We analyzed tomographic slices of 3D volumes and 3D models in the control and *DG* CKO photoreceptor synapses (Fig. 5*A*–*F*). A normal rod synaptic terminus contains a single synaptic ribbon (Fig. 5*A*, labeled R), two horizontal cell processes (Fig. 5*A*, labeled H), and two rod bipolar dendrites (Fig. 5*A*, labeled B). In the photoreceptor ribbon synapse of the control mouse, the ribbon is located at the apex of an invagination, which accommodates the postsynaptic processes of bipolar and horizontal cells (Fig. 5*A*). We observed that dendritic terminals of horizontal cells were normally inserted into the invagination of the photoreceptor ribbon synapse in both the control and *DG* CKO retinas (Fig, 5*A*–*D*). In contrast, we found that the dendritic processes of bipolar cells were not inserted into the invagination of the rod photoreceptor ribbon synapses in the *DG* CKO retina (Fig. 5*B*,*D*,*F*). We also confirmed this using 3D models extracted from the tomograms (Fig. 5*E*,*F*). These results suggest that the loss of DG causes a structural defect of the synaptic connection between photoreceptors and bipolar cells. This structural defect of ribbon synapses in the *DG* CKO retina may underlie the abnormality of the ERG b-wave observed in the *DG* CKO mice.

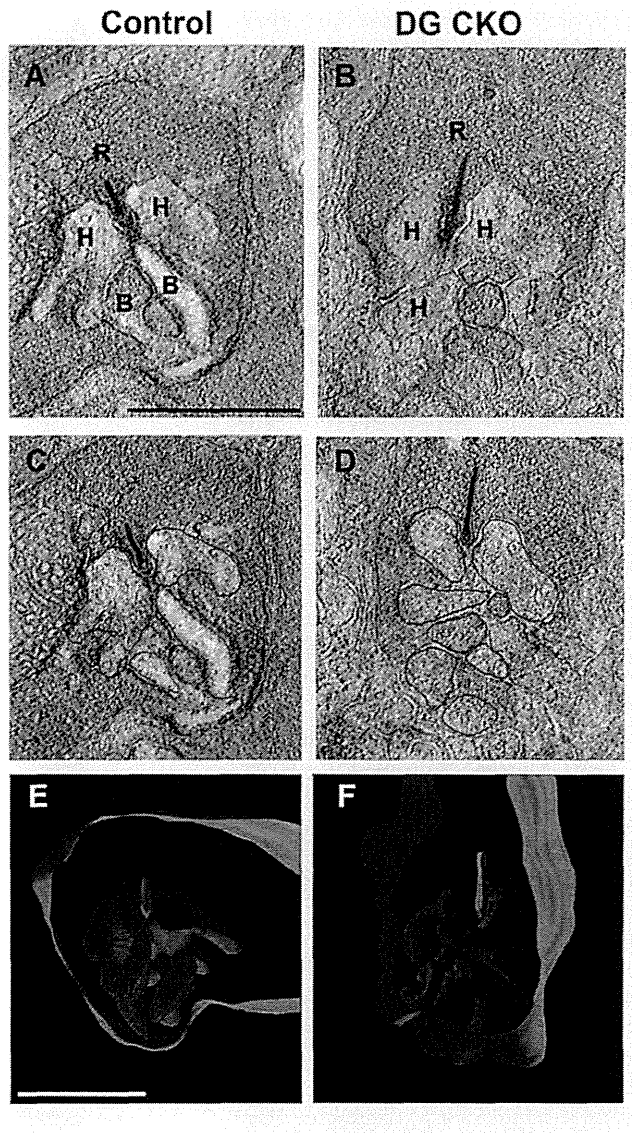

Figure 5. Electron microscopic analysis of the photoreceptor ribbon synapse in the *DG* CKO mice. Electron tomography of rod photoreceptor synapse terminals in the control (*A*, *C*, *E*) and *DG* CKO (*B*, *D*, *F*) retinas by ultrahigh-voltage electron microscopy. Synaptic ribbon (R), horizontal cell processes (H), and bipolar cell dendrites (B) are indicated in *A* and *B*. Representative demarcation of bipolar dendritic tips (magenta), horizontal processes (dark blue), ribbon (green), and rod plasma membrane (light blue) for tomography are shown for control (*C*) and *DG* CKO (*D*) retinas. Bipolar cells dendrites do not appose to the synaptic terminal in the rod photoreceptor ribbon synapse in the *DG* CKO retina (*B*, *D*, *F*). Scale bar represents 1 μm (*A*, *E*).

Pikachurin is important for the proper assembly of DG in the photoreceptor ribbon synapse

We found that DG is essential for the proper localization of Pikachurin in the photoreceptor synapse. Conversely, is Pikachurin necessary for the normal localization of DG? To address this issue, we examined the localization of DG in the adult *Pikachurin*$^{-/-}$ retina (Fig. 6*A–N'*). In the WT retina, Pikachurin localizes adjacent to synaptic ribbon (Fig. 6*A–A''*). We confirmed that the Pikachurin signal is completely lost in the *Pikachurin*$^{-/-}$ retina (percentage of Pikachurin$^+$ CtBP2$^+$ synapses in CtBP2$^+$ synapses, 96.7 ± 1.3% in WT, $n = 121$ from three animals, 0% in *Pikachurin*$^{-/-}$, $n = 154$ from three animals; $p < 0.01$) (Fig. 6*B–B''*) (Sato et al., 2008). Interestingly, we found that the DG signal in the OPL is severely depleted in *Pikachurin*$^{-/-}$ photoreceptor synapses compared with that in the control retina (percentage of DG$^+$ CtBP2$^+$ synapses in CtBP2$^+$ synapses, 95.7 ± 2.8% in WT, $n = 208$ from four animals, 15.5 ± 6.6% in *Pikachurin*$^{-/-}$, $n = 153$ from five animals; $p < 0.01$) (Fig. 6*C,D*). The DG signal loss is observed in both rod and cone photoreceptor synapses of the *Pikachurin*$^{-/-}$ retina compared with those of the control retina (Fig. 6*E–H'*). We previously showed that Pikachurin is expressed exclusively in photoreceptor cells and not in Müller glial cells (Sato et al., 2008). Consistent with this, the DG signals in blood vessels and the ILM of Müller glial endfeet are indistinguishable between the wild-type and *Pikachurin*$^{-/-}$ retinas (Fig. 6*I–J'*), suggesting that the ERG abnormality observed in the *Pikachurin*$^{-/-}$ mouse was not due to the defect of the DGC in Müller glial cells. Similar to the *DG* CKO retina, other photoreceptor synaptic markers including dystrophin and mGluR6 were unaffected in the *Pikachurin*$^{-/-}$ retina (percentage of dystrophin$^+$ mGluR6$^+$ puncta in mGluR6$^+$ puncta, 100% in WT, $n = 211$ from four animals, 100% in *Pikachurin*$^{-/-}$, $n = 205$ from five animals; percentage of mGluR6$^+$ CtBP2$^+$ synapses in CtBP2$^+$ synapses, 95.8 ± 2.7% in WT, $n = 156$ from three animals, 92.5 ± 2.2% in *Pikachurin*$^{-/-}$, $n = 111$ from three animals; $p > 0.05$) (Fig. 6*K–N'*). These results suggest that Pikachurin is required for the assembly of DG in photoreceptor synaptic terminals.

Pikachurin Laminin-G repeat domains are sufficient for DG clustering on the cell surface

In *Pikachurin*$^{-/-}$ photoreceptor ribbon synapses, we observed significantly de-

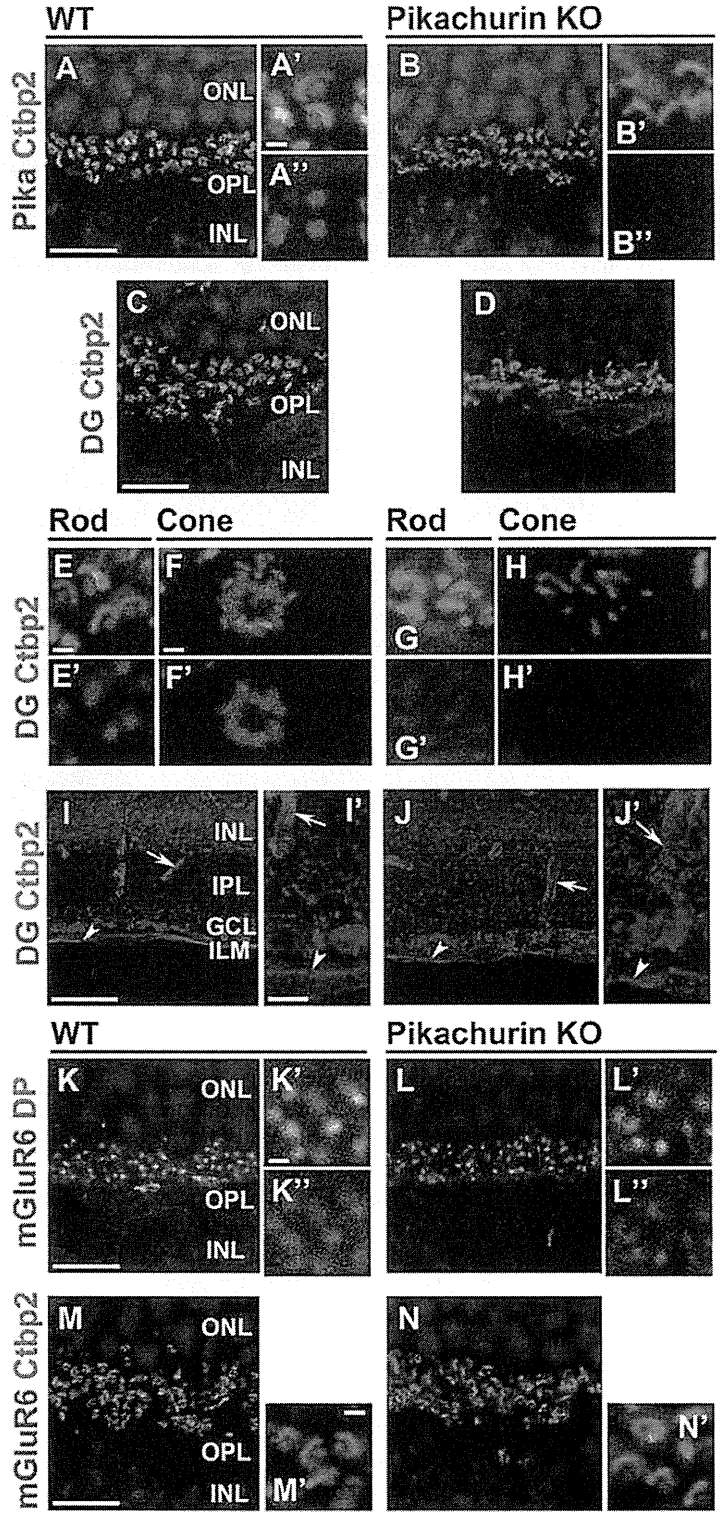

Figure 6. Pikachurin is required for the proper synaptic localization of DG in photoreceptor cells. Immunostaining of photoreceptor synaptic markers in the *Pikachurin*$^{-/-}$ retina. Retinal sections from control (*A–A''*, *C*, *E–F'*, *I*, *I'*, *K–K''*, *M*, *M'*) and *Pikachurin*$^{-/-}$ (*B–B''*, *D*, *G–H'*, *J*, *J'*, *L–L''*, *N*, *N'*) mice were stained with the antibodies against Pikachurin (red in *A–B''*), CtBP2 (green in *A–J'*, *M–N'*), DG (red in *C–J'*), dystrophin (green in *K–L''*), and mGluR6 (red in *K–N'*). Higher-magnification views of rod (*E*, *E'*, *G*, *G'*) and cone (*F*, *F'*, *H*, *H'*) photoreceptor ribbon synapses were shown. Higher-magnification views of *A*, *B*, *I*, *J*, *K*, *L*, *M*, and *N* are shown in *A'*, *A''*, *B'*, *B''*, *I'*, *J'*, *K'*, *K''*, *L'*, *L''*, *M'*, and *N'*, respectively. Nuclei were stained with DAPI (blue). Loss of the Pikachurin signal in the *Pikachurin*$^{-/-}$ OPL is shown (*B–B''*). DG signal is significantly decreased in both rod and cone photoreceptor synapses of *Pikachurin*$^{-/-}$ mice (*G-H'*), whereas the DG in blood vessels (arrows in *I*, *I'*, *J*, *J'*) and the ILM (arrowheads in *I*, *I'*, *J*, *J'*) are unaltered between WT and *Pikachurin*$^{-/-}$ retinas. Dystrophin, mGluR6 and CtBP2 signals are indistinguishable between WT and *Pikachurin*$^{-/-}$ retinas. Scale bars: *A*, *C*, *I'*, *K*, *M*, 10 μm; *I*, 50 μm; *A'*, *E*, *F*, *K'*, *M'*, 1 μm. IPL, inner plexiform layer.

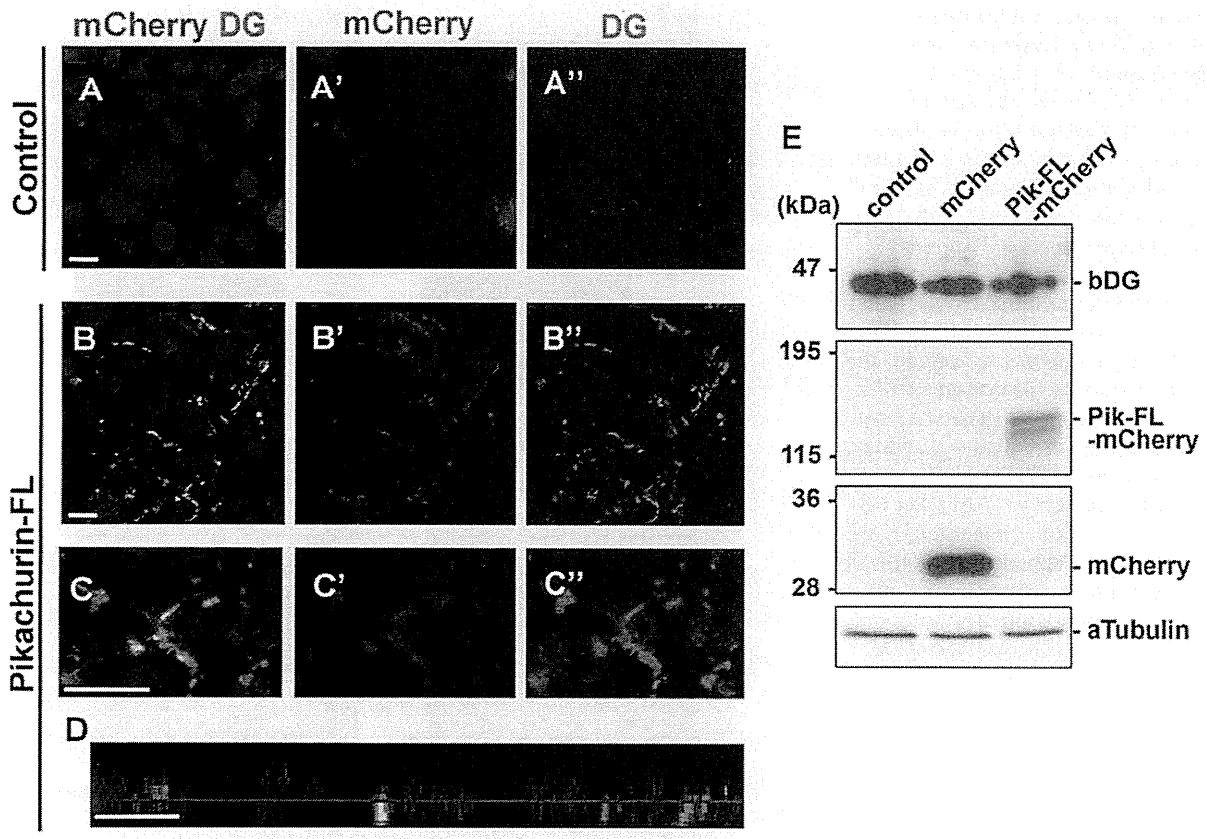

Figure 7. Overexpression of Pikachurin induces clustering of DG in HEK293 cells. HEK293 cells were transfected with a plasmid expressing mCherry (*A–A″*) or Pikachurin-FL-mCherry (*B–D*). mCherry (red) and β-dystroglycan (DG, green) signals were observed. Transverse (*A–C″*) or apical-basal (*D*) optical sections of cells are shown. Higher-magnification views of HEK293 cells transfected with the *Pikachurin-FL-mCherry* plasmid are shown (*C–C″*). DG clustering was observed at the cell–cell junction of cells transfected with the *Pikachurin-FL-mCherry* expression plasmid. Nuclei were stained with DAPI (blue). *E*, Western blots were performed to examine the amount of DG in cells. No obvious change of DG amount was observed in the cells expressing Pikachurin or mCherry alone. Scale bars, 10 μm.

creased DG signals. This result suggests that Pikachurin is necessary for the proper assembly of DG in the photoreceptor ribbon synapse. Pikachurin may regulate the DG clustering on cell surfaces through direct interaction. To examine this possibility, we overexpressed Pikachurin in HEK293 cells, which endogenously express DG, and observed the localization change of endogenous DG by immunostaining (Fig. 7*A–D*). HEK293 cells were transfected with plasmids expressing *mCherry* tagged with full-length *Pikachurin* (*Pikachurin-FL-mCherry*) or *mCherry* only as a control, and stained with an anti-DG antibody. In the cells transfected with a control plasmid, we observed no obvious accumulation of the DG signal (Fig. 7*A–A″*). However, in the cells transfected with plasmids expressing *Pikachurin-FL-mCherry*, we found a concentrated DG signal in cell–cell junctions (Fig. 7*B–D*). Notably, an mCherry-tagged Pikachurin signal was enriched and clustered in cell–cell junctions together with the DG signal (Fig. 7*B–D*). This result shows that Pikachurin is sufficient to assemble DG on the cell surface. At the same time, this result suggests that the expression of Pikachurin induces the formation of the DG–Pikachurin complex on the cell surface. To test whether the total DG amount in the cells changes or not, we performed Western blots and analyzed the amount of DG in the cells. We observed no obvious change of DG protein amount between the cells transfected with the mCherry control and Pikachurin constructs (Fig. 7*E*). Overexpression of Pikachurin does not seem to induce the expression or degradation of DG.

To determine the critical domain of the Pikachurin protein for DG clustering on the cell surface, we prepared plasmids expressing various Pikachurin deletion constructs and transfected them into HEK293 cells (Fig. 8*A–I*). We observed significant DG clusterings in the cells transfected with plasmids expressing Pikachurin deletion constructs with LG2–3 domains (Pik-FL, Pik-LG1–3, Pik-LG2–3, Pik-FN-LG) (Fig. 8*B–E′*), whereas no DG clustering was detected in the cells transfected with plasmids expressing Pikachurin without the LG2–3 domains (Pik-FN, Pik-LG3, SS-mCherry) (Fig. 8*F–H′*). This result suggests that the Pikachurin LG2–3 domains are necessary to induce DG clustering on the cell surface, and that the LG2–3 domains were core regions for the formation of the DG–Pikachurin complex.

Discussion

Photoreceptor DG is required for normal retinal physiology

In the current study, we investigated the functional role of DG in the retinal photoreceptor synaptic terminus. Attenuation of ERGs is observed in both MD patients and the corresponding model animals. In the mouse retina, DG is expressed in photoreceptor ribbon synapses in the OPL and Müller glial endfeet in the ILM and blood vessels (Schmitz and Drenckhahn, 1997b; Ueda et al., 2000; Blank et al., 2002). Since DG is detected in multiple areas of the retina, it was unclear which part of the defect is responsible for the ERG abnormality in MD patients and MD model animals. A recent study reported that mice with condi-

tional deletions of DG in Müller glial cells using *Nestin-Cre* and *GFAP-Cre* showed a loss of DG from the ILM but maintained DG expression in the OPL (Satz et al., 2009). These mice showed weakly reduced ERG b-wave amplitudes, but no obvious prolongation of b-wave implicit time was observed (Satz et al., 2009). Although previous studies reported that DG and/or Pikachurin-positive puncta were reduced in *DG* CKO/*Nestin-Cre* mice, it is still unclear whether or not the photoreceptor-specific loss of DG causes physiological dysfunction (Satz et al., 2009; Hu et al., 2011). In this study, we demonstrated that the mice lacking DG in photoreceptors showed a severe reduction of ERG b-wave amplitude with marked prolongation of b-wave implicit time, suggesting that photoreceptor synaptic DG is critical for both the amplitude and implicit time of the b-wave. In addition, we also showed that deficiency of Pikachurin does not cause the loss of DG from Müller glial endfeet. This result also supports evidence that the loss of the DGC in the OPL can cause attenuation of ERGs, since *Pikachurin*$^{-/-}$ mice also showed ERG attenuation (Sato et al., 2008). Our results in this study and observations from previous studies suggest that prolonged b-wave implicit time in MD model mice is most likely due to the functional defect of DGC formation in photoreceptor synapses. However, our study did not exclude the possibility that the DGC defect expressed in cells other than photoreceptors contributes to the ERG attenuation observed in MD patients and MD animal models.

Several studies by immunoelectron microscopic analysis have shown that DG localizes in photoreceptor presynapses but not in the postsynaptic dendritic tips of bipolar or horizontal cells (Schmitz and Drenckhahn, 1997a; Ueda et al., 1998; Blank et al., 1999; Jastrow et al., 2006). We observed a loss of invagination in bipolar processes but not in horizontal processes in *DG* CKO photoreceptor synapses. Why does the DG defect not affect the structure of horizontal processes? One possibility is that DG has a redundant factor in the horizontal process invagination, but not in the formation of bipolar processes. In mice, invagination of horizontal processes into photoreceptor synapses occurs between P7 and P10, whereas invagination of bipolar processes begins later, mainly between P10 and P14 (Blanks et al., 1974). A redundant factor for DG may function around P7–P10 in horizontal process invagination. Another possibility is that the molecular mechanism of invagination is totally different for horizontal and bipolar processes. An unknown molecular system independent from the DG–Pikachurin system may regulate horizontal process invagination.

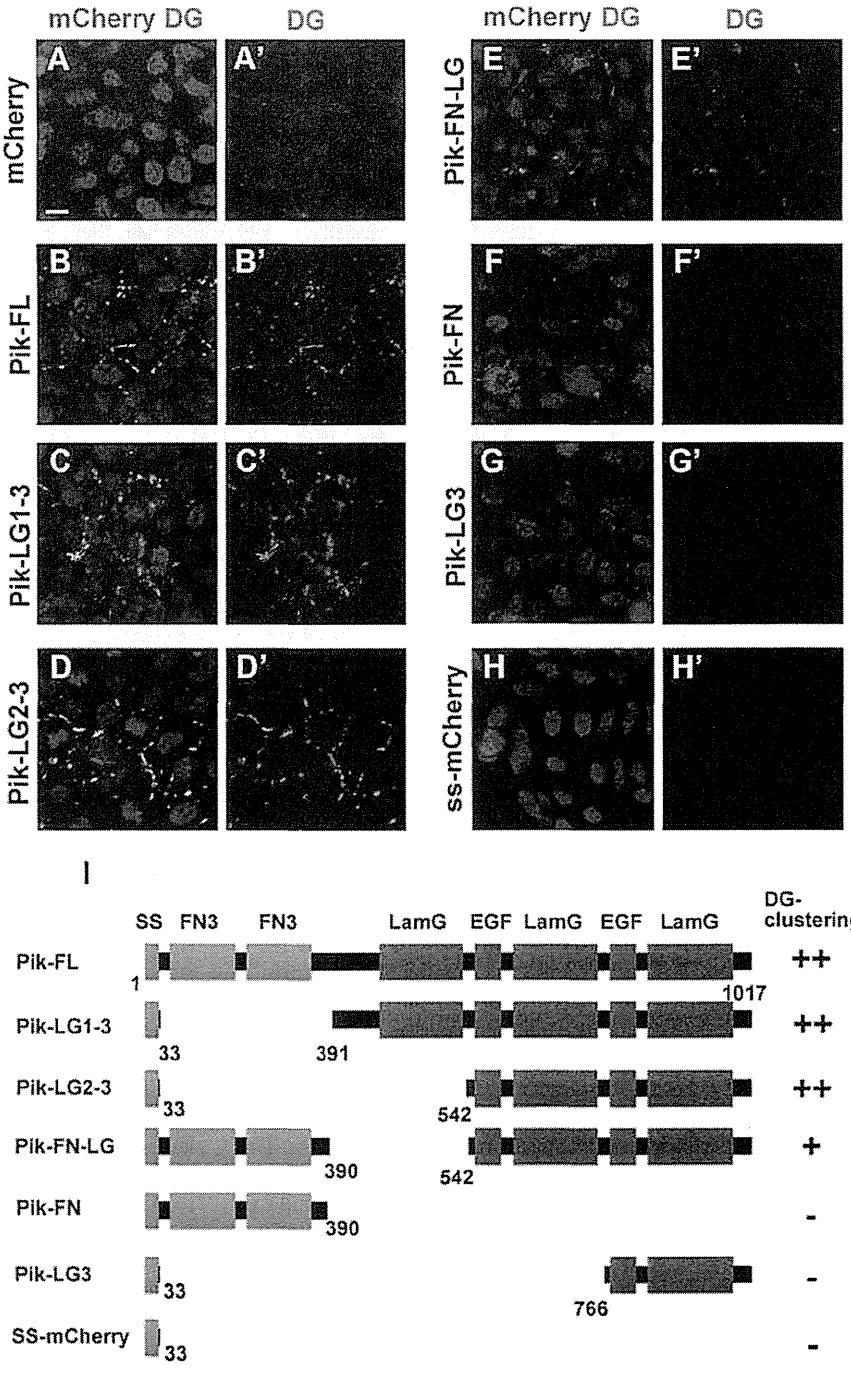

Figure 8. Laminin G repeats of Pikachurin are essential for the assembly of the DG–Pikachurin complex on the cell surface. *A–H'*, HEK293 cells were transfected with plasmids expressing various Pikachurin-deletion constructs. Seventy-two hours after transfection, subcellular localization of DG (green) and mCherry-tagged Pikachurin-deletion proteins (red) was observed. Nuclei were stained with DAPI (blue). Scale bar represents 10 μm. *I*, A schematic diagram of Pikachurin deletion constructs fused with mCherry at their C terminus. Amino acid numbers are shown at the bottom of each construct. DG clustering was observed in cells transfected with plasmids expressing Pikachurin deletion constructs with LG2–3 domains (Pik-FL, Pik-LG1–3, Pik-LG2–3, Pik-FN-LG), whereas no DG clustering was detected in the cells transfected with plasmids expressing Pikachurin constructs without LG2–3 domains.

Interaction of Pikachurin with DG induces DG clustering on the cell surface

Previous biochemical studies showed a direct interaction of DG and Pikachurin *in vitro* (Sato et al., 2008; Kanagawa et al., 2010), however, their functional interaction *in vivo* had not been well examined. In the current study, we provided several lines of evidence for the interaction between Pikachurin and DG *in vivo*.

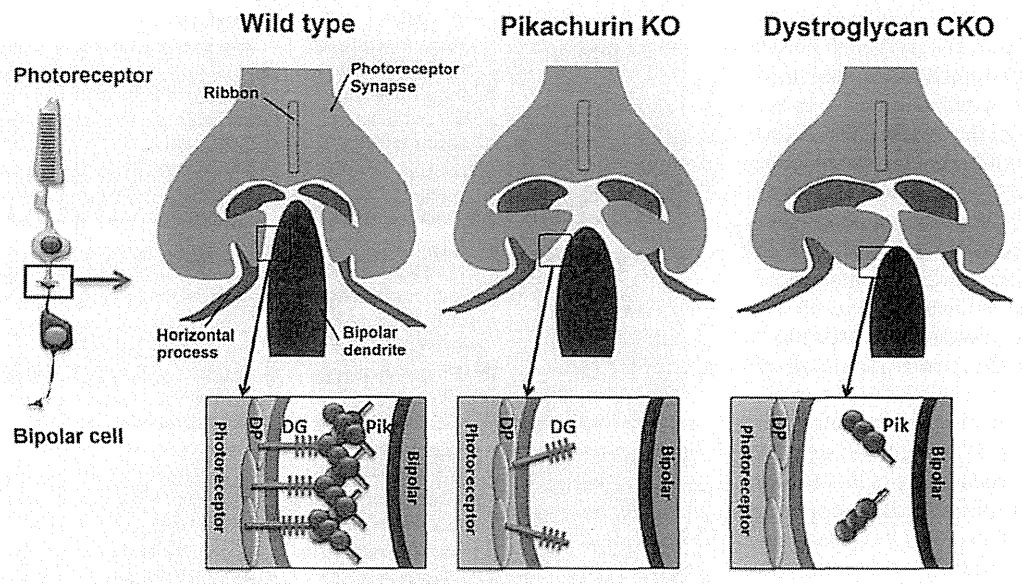

Figure 9. A hypothetical model of DG and Pikachurin function in photoreceptor synaptic terminals. Schematic diagrams of synaptic structures (top) and molecular interaction (bottom) in the WT (left), *Pikachurin* KO (middle) and *DG* CKO (right) retinas are shown. Left, In the WT retina, Pikachurin molecules form oligomers through their Laminin G domains. Oligomerization of Pikachurin induces the clustering of DG on the photoreceptor synaptic surface of the WT retina. Middle, In the *Pikachurin*$^{-/-}$ retina DG clustering at the synaptic terminal is not induced because of the loss of DG interaction with oligomerized Pikachurin. Lack of DG clustering at the photoreceptor synaptic tip causes a defect of synaptic connection between photoreceptors and bipolar cells, resulting in the abnormal ERGs observed in the *Pikachurin*$^{-/-}$ mice. Right, In the *DG* CKO retina, loss of DG prevents Pikachurin accumulation on the tips of photoreceptor synapses. Lack of DG in the synaptic terminal causes a more severe defect in the structure of photoreceptor synapses.

First, conditional deletion of DG in the photoreceptor presynaptic region causes a defect of Pikachurin localization in photoreceptor synapses, the prolongation of both ERG amplitude and implicit time, and a defect of synaptic ultrastructures between photoreceptors and bipolar cells. Second, the loss of Pikachurin affects proper DG assembly in the photoreceptor ribbon synapse. Third, expression of the DG binding domains of Pikachurin in cultured cells causes the clustering of DG on the cell surface. These results strongly support the idea that the interaction between DG and Pikachurin is essential for the formation of proper synaptic structure of photoreceptors.

In this study, we found that the forced expression of Pikachurin in cultured cells causes DG clustering on the cell surface. This result suggests that the interaction between Pikachurin and DG triggers assembly of the DG–Pikachurin complex on the cell surface. What is the molecular mechanism for the formation of this complex? One possibility is that Pikachurin oligomerization induces the assembly of the DG–Pikachurin complex. Previously we showed that Pikachurin is able to form oligomeric structures through LG repeats (Kanagawa et al., 2010). This suggests a molecular mechanism underlying the clustering of the DG–Pikachurin complex in the photoreceptor synapse; both the oligomerization of Pikachurin and the interaction of Pikachurin with DG cause the clustering of the DG–Pikachurin complex on the cell surface, thus, the DG–Pikachurin complex accumulates on the cell surface (Fig. 9). Interestingly, other DG interacting proteins including agrin, laminin, perlecan and neurexin also contain LG/EGF repeats (Ervasti and Campbell, 1993; Gee et al., 1994; Peng et al., 1998; Sugita et al., 2001). DG clustering by DG-interacting proteins may be regulated by a common molecular mechanism through the LG repeat domains.

Notably, the abnormality of both amplitudes and implicit times of ERGs in the *DG* CKO mice were more severe than in the *Pikachurin*$^{-/-}$ mice, suggesting that DG is more critical for photoreceptor synapse formation than Pikachurin. Consistent with our hypothesis, the DG signal was significantly reduced in photoreceptor synapses in the *Pikachurin*$^{-/-}$ OPL. However, a slight amount of DG remains in photoreceptor synapses in the *Pikachurin*$^{-/-}$ retina. There are two possible explanations for the phenotype difference between the loss of DG and the loss of Pikachurin. The first possible explanation is that DG is relatively stable even without interacting with Pikachurin. In this case, the structural change of the photoreceptor synapse caused by the loss of Pikachurin may be milder than that caused by the loss of DG, resulting in a milder ERG attenuation in the *Pikachurin*$^{-/-}$ mice than that in the *DG* CKO mice. The second explanation is that DG also interacts with other extracellular matrix proteins in addition to Pikachurin, and this additional interaction partially keeps DG anchored on the photoreceptor synaptic surface without the DG–Pikachurin interaction. DG in the photoreceptor synapse may interact with other DG ligands including laminin, agrin, neurexin, perlecan, or uncharacterized ECM proteins.

In *Drosophila*, a Laminin G repeats-containing protein, spacemaker, is required for the generation of inter-rhabdomeral space, a small extracellular space among photoreceptor rhabdomers in the compound eyes (Zelhof et al., 2006). Interestingly, the amino acid sequence of the spacemaker Laminin G repeats is very similar to that of Pikachurin. It is possible that Pikachurin-like Laminin G domains may have the ability to expand and/or keep small extracellular space, such as photoreceptor synaptic cleft and inter-rhabdomeral space by oligomerization or interaction with other ECM proteins. Our observations in the current study suggest that the DG–Pikachurin complex regulates the formation of the fine structures of the synaptic terminal, what we called "micromorphogenesis" of the synaptic terminal.

A recent report showed that postsynaptic DG regulates presynaptic neurotransmitter release at the *Drosophila* NMJ (Bogdanik et al., 2008). Together with our observation, the loss of DG might affect the structure not only on the presynaptic side where DG localizes, but also on the postsynaptic side. Although we observed no obvious defects of mGluR6 distribution in the postsynapse of bipolar dendritic terminals in the OPL, we do not

exclude the possibility that the loss of DG or Pikachurin affects the structure and/or the molecular composition of the postsynapse of bipolar terminals.

In summary, our findings demonstrate that photoreceptor DG is essential for the structural formation of the photoreceptor synapse and physiological synaptic connection between photoreceptor and bipolar cells. In addition, the loss of DG notably decreased the Pikachurin localization in photoreceptor synapses. We found that loss of Pikachurin in the photoreceptor synapse causes the depletion of DG at photoreceptor synapses. Furthermore, we observed that overexpression of Pikachurin in cultured cells induces formation of the DG–Pikachurin complex and facilitates the clustering of DG on the cell surface. These results suggest that Pikachurin is necessary and sufficient for DG assembly on the cell membrane, and for the functional link between Pikachurin and DG in photoreceptor synaptic formation. The micromorphogenesis mechanism observed in the DG–Pikachurin interaction in the photoreceptor-bipolar synapse formation may also be observed in the interaction between other LG-containing DG ligands and DG in other synapses and tissues.

References

Beltrán-Valero de Bernabé D, Currier S, Steinbrecher A, Celli J, van Beusekom E, van der Zwaag B, Kayserili H, Merlini L, Chitayat D, Dobyns WB, Cormand B, Lehesjoki AE, Cruces J, Voit T, Walsh CA, van Bokhoven H, Brunner HG (2002) Mutations in the *O*-mannosyltransferase gene POMT1 give rise to the severe neuronal migration disorder Walker-Warburg syndrome. Am J Hum Genet 71:1033–1043.

Blank M, Koulen P, Blake DJ, Kröger S (1999) Dystrophin and beta-dystroglycan in photoreceptor terminals from normal and mdx3Cv mouse retinae. Eur J Neurosci 11:2121–2133.

Blank M, Blake DJ, Kröger S (2002) Molecular diversity of the dystrophin-like protein complex in the developing and adult avian retina. Neuroscience 111:259–273.

Blanks JC, Adinolfi AM, Lolley RN (1974) Synaptogenesis in the photoreceptor terminal of the mouse retina. J Comp Neurol 156:81–93.

Bogdanik L, Framery B, Frölich A, Franco B, Mornet D, Bockaert J, Sigrist SJ, Grau Y, Parmentier ML (2008) Muscle dystroglycan organizes the postsynapse and regulates presynaptic neurotransmitter release at the *Drosophila* neuromuscular junction. PLoS One 3:e2084.

Brockington M, Blake DJ, Prandini P, Brown SC, Torelli S, Benson MA, Ponting CP, Estournet B, Romero NB, Mercuri E, Voit T, Sewry CA, Guicheney P, Muntoni F (2001) Mutations in the fukutin-related protein gene (FKRP) cause a form of congenital muscular dystrophy with secondary laminin alpha2 deficiency and abnormal glycosylation of alpha-dystroglycan. Am J Hum Genet 69:1198–1209.

Carter-Dawson LD, LaVail MM (1979) Rods and cones in the mouse retina. I. Structural analysis using light and electron microscopy. J Comp Neurol 188:245–262.

Chen S, Kadomatsu K, Kondo M, Toyama Y, Toshimori K, Ueno S, Miyake Y, Muramatsu T (2004) Effects of flanking genes on the phenotypes of mice deficient in basigin/CD147. Biochem Biophys Res Commun 324:147–153.

Cibis GW, Fitzgerald KM, Harris DJ, Rothberg PG, Rupani M (1993) The effects of dystrophin gene mutations on the ERG in mice and humans. Invest Ophthalmol Vis Sci 34:3646–3652.

D'Souza VN, Nguyen TM, Morris GE, Karges W, Pillers DA, Ray PN (1995) A novel dystrophin isoform is required for normal retinal electrophysiology. Hum Mol Genet 4:837–842.

Ervasti JM, Campbell KP (1993) A role for the dystrophin-glycoprotein complex as a transmembrane linker between laminin and actin. J Cell Biol 122:809–823.

Fitzgerald KM, Cibis GW, Giambrone SA, Harris DJ (1994) Retinal signal transmission in Duchenne muscular dystrophy: evidence for dysfunction in the photoreceptor/depolarizing bipolar cell pathway. J Clin Invest 93:2425–2430.

Furukawa A, Koike C, Lippincott P, Cepko CL, Furukawa T (2002) The mouse Crx 5′-upstream transgene sequence directs cell-specific and developmentally regulated expression in retinal photoreceptor cells. J Neurosci 22:1640–1647.

Gee SH, Montanaro F, Lindenbaum MH, Carbonetto S (1994) Dystroglycan-alpha, a dystrophin-associated glycoprotein, is a functional agrin receptor. Cell 77:675–686.

Haenggi T, Fritschy JM (2006) Role of dystrophin and utrophin for assembly and function of the dystrophin glycoprotein complex in non-muscle tissue. Cell Mol Life Sci 63:1614–1631.

Henry MD, Campbell KP (1996) Dystroglycan: an extracellular matrix receptor linked to the cytoskeleton. Curr Opin Cell Biol 8:625–631.

Hoffman EP, Kunkel LM (1989) Dystrophin abnormalities in Duchenne/Becker muscular dystrophy. Neuron 2:1019–1029.

Hu H, Li J, Zhang Z, Yu M (2011) Pikachurin interaction with dystroglycan is diminished by defective *O*-mannosyl glycosylation in congenital muscular dystrophy models and rescued by LARGE overexpression. Neurosci Lett 489:10–15.

Ibraghimov-Beskrovnaya O, Ervasti JM, Leveille CJ, Slaughter CA, Sernett SW, Campbell KP (1992) Primary structure of dystrophin-associated glycoproteins linking dystrophin to the extracellular matrix. Nature 355:696–702.

Jastrow H, Koulen P, Altrock WD, Kröger S (2006) Identification of a beta-dystroglycan immunoreactive subcompartment in photoreceptor terminals. Invest Ophthalmol Vis Sci 47:17–24.

Kanagawa M, Omori Y, Sato S, Kobayashi K, Miyagoe-Suzuki Y, Takeda S, Endo T, Furukawa T, Toda T (2010) Post-translational maturation of dystroglycan is necessary for pikachurin binding and ribbon synaptic localization. J Biol Chem 285:31208–31216.

Kobayashi K, Nakahori Y, Miyake M, Matsumura K, Kondo-Iida E, Nomura Y, Segawa M, Yoshioka M, Saito K, Osawa M, Hamano K, Sakakihara Y, Nonaka I, Nakagome Y, Kanazawa I, Nakamura Y, Tokunaga K, Toda T (1998) An ancient retrotransposal insertion causes Fukuyama-type congenital muscular dystrophy. Nature 394:388–392.

Koike C, Obara T, Uriu Y, Numata T, Sanuki R, Miyata K, Koyasu T, Ueno S, Funabiki K, Tani A, Ueda H, Kondo M, Mori Y, Tachibana M, Furukawa T (2010) TRPM1 is a component of the retinal ON bipolar cell transduction channel in the mGluR6 cascade. Proc Natl Acad Sci U S A 107:332–337.

Kremer JR, Mastronarde DN, McIntosh JR (1996) Computer visualization of three-dimensional image data using IMOD. J Struct Biol 116:71–76.

Lee Y, Kameya S, Cox GA, Hsu J, Hicks W, Maddatu TP, Smith RS, Naggert JK, Peachey NS, Nishina PM (2005) Ocular abnormalities in Large(myd) and Large(vls) mice, spontaneous models for muscle, eye, and brain diseases. Mol Cell Neurosci 30:160–172.

Liu J, Ball SL, Yang Y, Mei P, Zhang L, Shi H, Kaminski HJ, Lemmon VP, Hu H (2006) A genetic model for muscle-eye-brain disease in mice lacking protein *O*-mannose 1,2-*N*-acetylglucosaminyltransferase (POMGnT1). Mech Dev 123:228–240.

Longman C, Brockington M, Torelli S, Jimenez-Mallebrera C, Kennedy C, Khalil N, Feng L, Saran RK, Voit T, Merlini L, Sewry CA, Brown SC, Muntoni F (2003) Mutations in the human LARGE gene cause MDC1D, a novel form of congenital muscular dystrophy with severe mental retardation and abnormal glycosylation of alpha-dystroglycan. Hum Mol Genet 12:2853–2861.

Moore SA, Saito F, Chen J, Michele DE, Henry MD, Messing A, Cohn RD, Ross-Barta SE, Westra S, Williamson RA, Hoshi T, Campbell KP (2002) Deletion of brain dystroglycan recapitulates aspects of congenital muscular dystrophy. Nature 418:422–425.

Nishida A, Furukawa A, Koike C, Tano Y, Aizawa S, Matsuo I, Furukawa T (2003) Otx2 homeobox gene controls retinal photoreceptor cell fate and pineal gland development. Nat Neurosci 6:1255–1263.

Peng HB, Ali AA, Daggett DF, Rauvala H, Hassell JR, Smalheiser NR (1998) The relationship between perlecan and dystroglycan and its implication in the formation of the neuromuscular junction. Cell Adhes Commun 5:475–489.

Pillers DA, Bulman DE, Weleber RG, Sigesmund DA, Musarella MA, Powell BR, Murphey WH, Westall C, Panton C, Becker LE, Worton RG, Ray PN (1993) Dystrophin expression in the human retina is required for normal function as defined by electroretinography. Nat Genet 4:82–86.

Pillers DA, Weleber RG, Woodward WR, Green DG, Chapman VM, Ray PN (1995) mdxCv3 mouse is a model for electroretinography of Duchenne/Becker muscular dystrophy. Invest Ophthalmol Vis Sci 36:462–466.

Robson JG, Frishman LJ (1995) Response linearity and kinetics of the cat retina: the bipolar cell component of the dark-adapted electroretinogram. Vis Neurosci 12:837–850.

Robson JG, Frishman LJ (1996) Photoreceptor and bipolar cell contributions to the cat electroretinogram: a kinetic model for the early part of the flash response. J Opt Soc Am A Opt Image Sci Vis 13:613–622.

Sato S, Omori Y, Katoh K, Kondo M, Kanagawa M, Miyata K, Funabiki K, Koyasu T, Kajimura N, Miyoshi T, Sawai H, Kobayashi K, Tani A, Toda T, Usukura J, Tano Y, Fujikado T, Furukawa T (2008) Pikachurin, a dystroglycan ligand, is essential for photoreceptor ribbon synapse formation. Nat Neurosci 11:923–931.

Satz JS, Philp AR, Nguyen H, Kusano H, Lee J, Turk R, Riker MJ, Hernández J, Weiss RM, Anderson MG, Mullins RF, Moore SA, Stone EM, Campbell KP (2009) Visual impairment in the absence of dystroglycan. J Neurosci 29:13136–13146.

Schmitz F, Drenckhahn D (1997a) Localization of dystrophin and beta-dystroglycan in bovine retinal photoreceptor processes extending into the postsynaptic dendritic complex. Histochem Cell Biol 108:249–255.

Schmitz F, Drenckhahn D (1997b) Dystrophin in the retina. Prog Neurobiol 53:547–560.

Sugita S, Saito F, Tang J, Satz J, Campbell K, Südhof TC (2001) A stoichiometric complex of neurexins and dystroglycan in brain. J Cell Biol 154:435–445.

Takaoka A, Hasegawa T, Yoshida K, Mori H (2008) Microscopic tomography with ultra-HVEM and applications. Ultramicroscopy 108:230–238.

tom Dieck S, Brandstätter JH (2006) Ribbon synapses of the retina. Cell Tissue Res 326:339–346.

Ueda H, Gohdo T, Ohno S (1998) Beta-dystroglycan localization in the photoreceptor and Muller cells in the rat retina revealed by immunoelectron microscopy. J Histochem Cytochem 46:185–191.

Ueda H, Baba T, Ohno S (2000) Current knowledge of dystrophin and dystrophin-associated proteins in the retina. Histol Histopathol 15:753–760.

van Reeuwijk J, Janssen M, van den Elzen C, Beltran-Valero de Bernabé D, Sabatelli P, Merlini L, Boon M, Scheffer H, Brockington M, Muntoni F, Huynen MA, Verrips A, Walsh CA, Barth PG, Brunner HG, van Bokhoven H (2005) POMT2 mutations cause alpha-dystroglycan hypoglycosylation and Walker-Warburg syndrome. J Med Genet 42:907–912.

Yoshida A, Kobayashi K, Manya H, Taniguchi K, Kano H, Mizuno M, Inazu T, Mitsuhashi H, Takahashi S, Takeuchi M, Herrmann R, Straub V, Talim B, Voit T, Topaloglu H, Toda T, Endo T (2001) Muscular dystrophy and neuronal migration disorder caused by mutations in a glycosyltransferase, POMGnT1. Dev Cell 1:717–724.

Zelhof AC, Hardy RW, Becker A, Zuker CS (2006) Transforming the architecture of compound eyes. Nature 443:696–699.

Clinical Ophthalmology

Dovepress
open access to scientific and medical research

Open Access Full Text Article

CASE REPORT

Peripheral capillary nonperfusion and full-field electroretinographic changes in eyes with frosted branch-like appearance retinal vasculitis

Yoshitsugu Matsui
Hideyuki Tsukitome
Eriko Uchiyama
Yuko Wada
Tatsuya Yagi
Hisashi Matsubara
Mineo Kondo

Department of Ophthalmology, Mie University Graduate School of Medicine, Tsu, Japan

Abstract: We report a patient with frosted branch-like appearance retinal vasculitis associated with peripheral capillary nonperfusion and full-field electroretinographic changes. A 62-year-old man presented with sudden bilateral decreased vision accompanied by headaches. His best-corrected visual acuity was 0.01 in both eyes. Fundus examination and fluorescein angiography showed bilateral frosted branch-like appearance retinal vasculitis, and spectral-domain optical coherence tomography showed severe macular edema in both eyes. The cerebrospinal fluid analyses showed an increased lymphocyte count and protein levels. He was treated with systemic corticosteroid therapy, and his best-corrected visual acuity improved to 0.8 OD and 1.0 OS at 6 months after onset. However, fluorescein angiography showed a lack of capillary perfusion in the periphery, and the oscillatory potentials on full-field electroretinography were severely reduced in both eyes. These findings indicated extensive retinal ischemia and inner retinal dysfunction, and that fluorescein angiography and full-field electroretinograms can be useful during follow-up of eyes with frosted branch-like appearance retinal vasculitis.

Keywords: frosted branch angiitis, aseptic meningitis, optical coherence tomography, electroretinogram, oscillatory potentials

Introduction

Frosted branch angiitis[1] is a rare type of periphlebitis characterized by white sheathing of the retinal vessels in association with different types of inflammatory eye disease.[2–4] The onset of frosted branch angiitis is usually sudden, and patients may complain of painless blurred vision, a central blind area, floaters, and photopsias.

Most patients with frosted branch angiitis respond to systemic corticosteroid therapy with good recovery of visual acuity, but various adverse complications have also been reported. These complications include macular scarring, retinal vein or artery occlusion, macular epiretinal membrane formation, diffuse retinal fibrosis, optic disc atrophy, peripheral capillary nonperfusion, and vitreous hemorrhage, all of which have been reviewed elsewhere.[3]

We report our findings in a 62-year-old man with bilateral frosted branch-like appearance retinal vasculitis accompanied by aseptic meningitis. He was treated with systemic corticosteroid therapy with good recovery of visual acuity. However, examinations at 6 months after onset revealed peripheral capillary nonperfusion and severe reduction of the amplitudes of oscillatory potentials on the electroretinogram. These changes suggested extensive retinal ischemia and inner retinal dysfunction, which required photocoagulation.

Correspondence: Mineo Kondo
Department of Ophthalmology, Mie University Graduate School of Medicine, 2-175 Edobashi, Tsu, 514-8507, Japan
Tel +815 9231 5027
Fax +815 9231 3036
Email mineo@clin.medic.mie-u.ac.jp

submit your manuscript | www.dovepress.com
Dovepress
http://dx.doi.org/10.2147/OPTH.S46118

Case report

A 62-year-old man presented with sudden bilateral decrease of vision accompanied by headaches. He did not have any systemic diseases, and his family history revealed no other members with eye disease. He had never experienced oral ulcers or skin lesions previously.

At our initial examination, his best-corrected visual acuity was 0.01 in both eyes, and Goldmann perimetry showed a severe central scotoma in both eyes. The intraocular pressure was 18 mmHg OD and 16 mmHg OS. Slit-lamp examination showed many fine keratic precipitates and cells in the aqueous and vitreous of both eyes. Severe sheathing of the retinal vessels and retinal hemorrhages was detected in both eyes by ophthalmoscopy (Figure 1, upper panel). Fluorescein angiography showed perivenous staining and leakage from the vessels (Figure 1, lower panel). Spectral-domain optical coherence tomography (Spectralis®, Heidelberg Engineering, Heidelberg, Germany) demonstrated severe macular edema with central macular thickness of 1045 μm OD and 991 μm OS (Figure 2, uppermost panel). We also recorded full-field electroretinograms and found that the amplitudes of the mixed rod and cone responses after dark adaptation were severely attenuated in both eyes (Figure 3, middle panel).

On systemic examination, blood count, biochemical analysis including kidney function tests, urine testing, and chest x-rays were within normal limits. Angiotensin-converting enzyme levels were also within normal limits. Tests for syphilis and human immunodeficiency virus were negative.

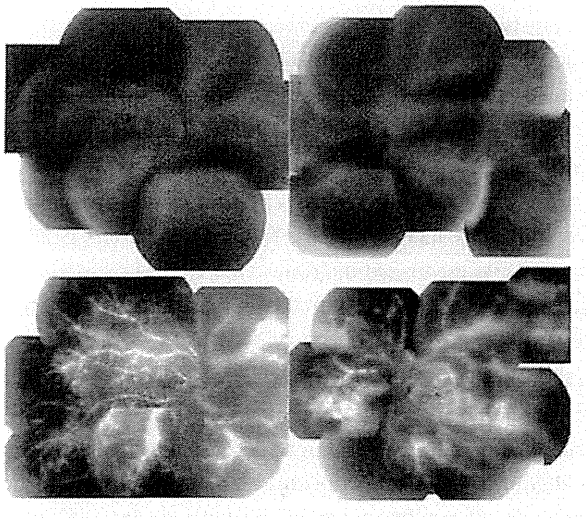

Figure 1 Fundus photographs and fluorescein angiograms at initial examination showing bilateral diffuse perivascular sheathing and retinal edema with intraretinal hemorrhages (upper panel).
Note: Fluorescein angiography shows extensive vascular leakage and retinal edema (lower panel).

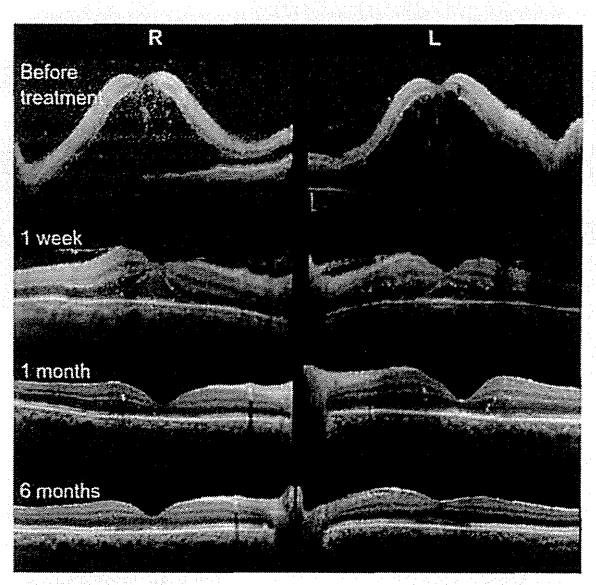

Figure 2 Changes in spectral-domain optical coherence tomograms at onset, and at one week, one month, and 6 months after treatment.

Lupus anticoagulant and anticardiolipin antibody were not detected. The HLA type was A11, A24, B39, B54, DR4, and DR8. Herpes simplex and varicella zoster IgG antibody titers suggested prior exposure only. Polymerase chain reaction analysis of the aqueous humor was negative for herpes simplex, herpes zoster, and cytomegalovirus DNA. Cerebrospinal fluid analysis disclosed an increased leukocyte count (72/mL, mononuclear cells) and protein level (49 mg/dL; normal 10–40 mg/dL). Cerebrospinal fluid cultures were negative.

Based on the results of these systemic examinations, we diagnosed our patient as having frosted branch-like appearance retinal vasculitis associated with aseptic meningitis. He was treated with pulsed steroid therapy (methylprednisolone 1000 mg/day × 3 days) followed by oral prednisolone (1 mg/kg/day), topical steroids, and mydriasis.

One month later, the patient's best-corrected visual acuity improved to 0.6 (OD) and 0.5 (OS), and spectral-domain optical coherence tomography showed a reduction in macular edema (Figure 2, third panel).

Six months after the start of steroid therapy, best-corrected visual acuity was improved to 0.8 OD and 1.0 OS and the fundus had returned to nearly normal (Figure 4, upper panel). Spectral-domain optical coherence tomography showed that the thickness of the retina was normal but the inner segment/outer segment junction of the photoreceptors was still disrupted at the fovea in both eyes (Figure 2, lowest panel). We performed fluorescein angiography again, and found that there were extensive areas without capillary perfusion in the

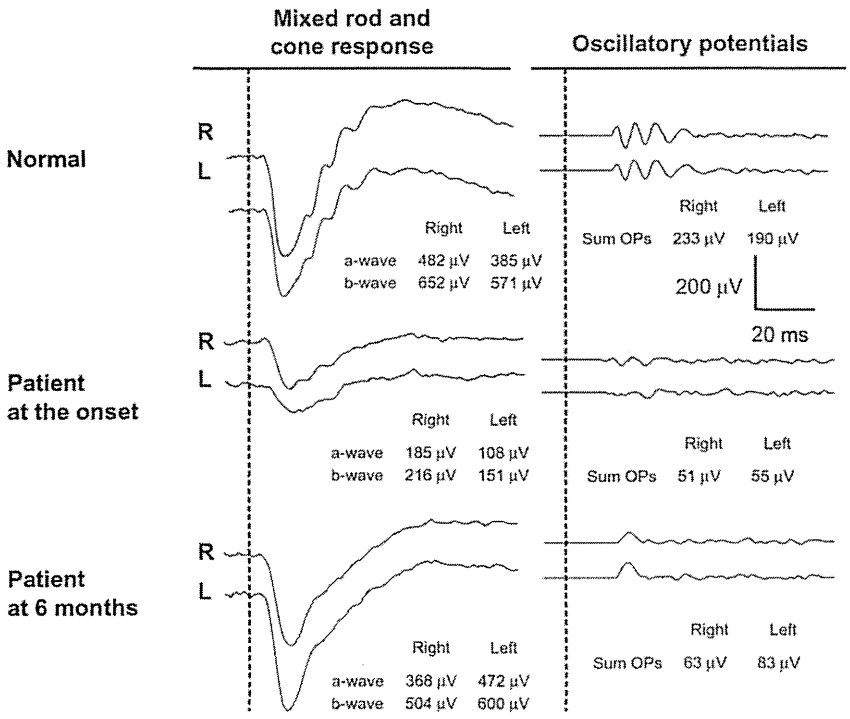

Figure 3 Changes in full-field electroretinograms.
Notes: Full-field mixed rod and cone electroretinograms were recorded after 20 minutes of dark adaptation at onset and 6 months after treatment. Full-field electroretinograms were elicited by a contact lens electrode with a built-in white light emitting diode (LE-2000, Tomey Co, Nagoya, Japan).[11] The stimulus intensity was 10.0 cd-s/m^2 (photopic units). Although the a-waves and b-waves recovered to normal, the oscillatory potentials were still severely reduced at 6 months after onset.

periphery of both eyes (Figure 4, lower panel). Full-field electroretinograms demonstrated nearly normal a waves and b waves, but severely reduced oscillatory potentials in both eyes (Figure 3, lowest panel). These results suggested extensive retinal ischemia and inner retinal dysfunction.

We then performed photocoagulation of the peripheral retina to prevent neovascularization and vitreous hemorrhage. There were no retinal complications in our patient during one year of follow-up after photocoagulation.

Discussion

Frosted branch angiitis is considered to be a clinical subtype of diffuse retinal periphlebitis and is associated with various types of systemic and ocular disease.[2–4] Frosted branch angiitis is reported to be associated with virus and bacterial infections, lymphoma, leukemia, Crohn's disease, systemic lupus, toxoplasmosis, Behçet's disease, central retinal vein occlusion, nephritis, and other systemic diseases.[2–4] The frosted branch-like appearance retinal vasculitis in our patient was believed to be associated with aseptic meningitis because he had headaches and an increased lymphocyte count and protein level in his cerebrospinal fluid. Further, no viral infection could be detected.

Johkura et al[5] reported a 20-year-old woman with frosted branch angiitis and aseptic meningitis who had headaches, nausea, and vomiting, and cerebrospinal fluid study showed lymphocyte counts increased to 83/mL and a protein level of 42 mg/dL. More recently, Chaume et al[6] reported an 11-year-old boy with frosted branch angiitis and aseptic meningitis. Their clinical findings and laboratory data were very similar to those in our patient.

In our patient, fluorescein angiography showed extensive areas without capillary perfusion in the peripheral retina and a selective reduction in amplitudes of the oscillatory potentials in both eyes. It is widely accepted that oscillatory potentials originate mainly from inhibitory neural pathways in the inner retina, including those of the amacrine and ganglion cells.[7] It has also been reported that a selective reduction in the amplitude of oscillatory potentials is also found when inner retinal function is extensively impaired, eg, in diabetic retinopathy or central retinal vein occlusion.[7] Thus, the findings of a lack of peripheral capillary perfusion and selective loss of oscillatory potentials on the electroretinogram in our patient strongly suggest that the retina was extensively ischemic and required photocoagulation. Luo et al[8] also used full-field electroretinograms during follow-up of a

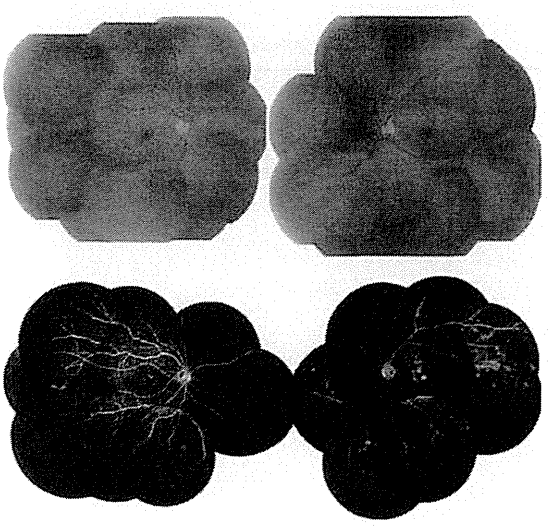

Figure 4 Fundus photographs and fluorescein angiograms 6 months after treatment.
Note: The fundus had recovered to nearly normal, but the fluorescein angiograms show extensive lack of capillary perfusion in the peripheral retina (lower panel).

5-year-boy with frosted branch angiitis, but reported that all electroretinographic components recovered to normal 6 months after treatment.

Our search using PubMed and the Japan Medical Abstracts Society yielded only three papers on frosted branch angiitis associated with peripheral capillary nonperfusion. In 1988, Kleiner et al[2] reported a 25-year-old man with frosted branch angiitis who developed multiple branch vein occlusion, capillary nonperfusion, and retinal neovascularization. In 1989, Terasaki et al[9] reported on a 21-year-old woman with frosted branch angiitis, who developed peripheral capillary nonperfusion and retinal neovascularization which required panretinal photocoagulation 18 months after onset. In 1993, Harigai et al[10] reported on a 39-year-old man with frosted branch angiitis who developed peripheral capillary nonperfusion at 7 months after onset. Despite panretinal photocoagulation, vitreous hemorrhages developed in his right eye. Although fluorescein angiography was repeatedly performed during follow-up, full-field electroretinograms were not recorded in these three patients.

The findings in our case suggest that extensive retinal ischemia and inner retinal dysfunction can occur in eyes with frosted branch-like appearance retinal vasculitis, and careful follow-up examinations are needed, even after good recovery of visual acuity. In addition to fluorescein angiography, full-field electroretinography may be useful during follow-up of these patients.

Acknowledgments

Funding for this work was received from the Ministry of Education, Culture, Science and Technology (23592603), Japan. The authors thank Duco I Hamasaki for editing the manuscript.

Disclosure

The authors report that they have no competing interests in this work.

References

1. Ito Y, Nakano M, Kyu N, Takeuchi M. Frosted branch angiitis in a child. *Rinsho Ganka*. 1976;30(7):797–803. Japanese.
2. Kleiner RC, Kaplan HJ, Shakin JL, Yannuzzi LA, Crosswell HH Jr, McLean WC Jr. Acute frosted retinal periphlebitis. *Am J Ophthalmol*. 1998;106(1):27–34.
3. Walker S, Iguchi A, Jones NP. Frosted branch angiitis: a review. *Eye (Lond)*. 2004;18(5):527–533.
4. Kleiner RC. Frosted branch angiitis: clinical syndrome or clinical sign? *Retina*. 1997;17(5):370–371.
5. Johkura K, Hara A, Hattori T, Hasegawa O, Kuroiwa Y. Frosted branch angitis associated with aseptic meningitis. *Eur J Neurol*. 2000;7(2):241.
6. Chaume A, Lemelle I, Chastagner P, Angioi K. A case report of frosted branch angiitis associated with aseptic meningitis in a young boy. *J Fr Ophtalmol*. 2011;34(2):129. e1–e5. French.
7. Wachtmeister L. Oscillatory potentials in the retina: what do they reveal. *Prog Retin Eye Res*. 1998;17(4):485–521.
8. Luo G, Yang P, Huang S, Jiang F, Wen F. A case report of frosted branch angiitis and its visual electrophysiology. *Doc Ophthalmol*. 1998–1999;97(2):135–142.
9. Terasaki H, Yanagida K, Tanaka T. An adult case of frosted branch angiitis with various systemic manifestation. *Folia Ophthalmol Jpn*. 1989;40(11):2438–2442. Japanese.
10. Harigai R, Seki R, Emi K, Oguro Y, Sato Y. A case of frosted branch angiitis associated with vitreous hemorrhage. *Folia Ophthalmol Jpn*. 1993;44(6):772–778. Japanese.
11. Kondo M, Piao CH, Tanikawa A, Horiguchi M, Miyake Y. A contact lens electrode with built-in high intensity white light-emitting diodes. *Doc Ophthalmol*. 2001;102(1):1–9.

Jpn J Ophthalmol (2012) 56:289–306
DOI 10.1007/s10384-012-0147-2

REVIEW

Retinal remodeling

B. W. Jones · M. Kondo · H. Terasaki · Y. Lin · M. McCall · R. E. Marc

Received: 26 January 2012 / Accepted: 18 March 2012 / Published online: 30 May 2012

Abstract Retinal photoreceptor degeneration takes many forms. Mutations in rhodopsin genes or disorders of the retinal pigment epithelium, defects in the adenosine triphosphate binding cassette transporter, ABCR gene defects, receptor tyrosine kinase defects, ciliopathies and transport defects, defects in both transducin and arrestin, defects in rod cyclic guanosine 3′,5′-monophosphate phosphodiesterase, peripherin defects, defects in metabotropic glutamate receptors, synthetic enzymatic defects, defects in genes associated with signaling, and many more can all result in retinal degenerative disease like retinitis pigmentosa (RP) or RP-like disorders. Age-related macular degeneration (AMD) and AMD-like disorders are possibly due to a constellation of potential gene targets and gene/gene interactions, while other defects result in diabetic retinopathy or glaucoma. However, all of these insults as well as traumatic insults to the retina result in retinal remodeling. Retinal remodeling is a universal finding subsequent to retinal degenerative disease that results in deafferentation of the neural retina from photoreceptor input as downstream neuronal elements respond to loss of input with negative plasticity. This negative plasticity is not passive in the face of photoreceptor degeneration, with a phased revision of retinal structure and function found at the molecular, synaptic, cell, and tissue levels involving all cell classes in the retina, including neurons and glia. Retinal remodeling has direct implications for the rescue of vision loss through bionic or biological approaches, as circuit revision in the retina corrupts any potential surrogate photoreceptor input to a remnant neural retina. However, there are a number of potential opportunities for intervention that are revealed through the study of retinal remodeling, including therapies that are designed to slow down photoreceptor loss, interventions that are designed to limit or arrest remodeling events, and optogenetic approaches that target appropriate classes of neurons in the remnant neural retina.

Keywords Retinal remodeling · Retina · Retinal degeneration · Retinitis pigmentosa · Macular degeneration

The content of this invited review article was presented at the ARVO-JOS joint symposium on April 15, 2010, held during the 114th Annual Meeting of the Japanese Ophthalmological Society.

B. W. Jones (✉) · Y. Lin · R. E. Marc
Department of Ophthalmology, Moran Eye Center, University of Utah, 65 Mario Capecchi Dr., Salt Lake City, UT 84132, USA
e-mail: bryan.jones@m.cc.utah.edu

M. Kondo · H. Terasaki
Department of Ophthalmology, Nagoya University, Graduate School of Medicine, Nagoya, Japan

M. McCall
Department of Ophthalmology and Visual Sciences, University of Louisville, Louisville, KY, USA

Introduction

Retinal remodeling as a consequence of retinal degenerative disease is an unavoidable phenomenon. A large number of investigators are engaged in exploring neural retinal remodeling as well as the therapeutic implications of retinal degenerations. The consensus is that the neural retina becomes reactive and is not passive in the face of photoreceptor degenerations. Furthermore, the substantial alterations now recognized as retinal remodeling occur from the molecular up through the synaptic, cellular, and

tissue levels [1–24], involving not only photoreceptors but all of the cell populations in the neural retina [1, 7, 9, 13, 18, 20–23, 25, 26].

Photoreceptor degeneration takes many forms that occur naturally in disease [27] and in conditions as far apart as trauma [28], the myriad forms of retinitis pigmentosa (RP) and RP-like disorders that are manifested through mutations in rhodopsin genes [16, 27, 29, 30], disorders of the retinal pigment epithelium (RPE) in Leber's congenital amaurosis [31–33], defects in the ATP-binding cassette transporter seen in Stargardt's disease [34–36], ABCR gene defects [37, 38], receptor tyrosine kinase defects [32, 39, 40], ciliopathies and transport defects [41, 42], defects in both transducin and arrestin [43–46], defects in rod cGMP phosphodiesterase [47–49], peripherin defects [50], defects in metabotropic glutamate receptors (mGluRs) [51, 52], synthetic enzymatic defects [53, 54], defects in genes associated with signaling [55–58], age-related macular degeneration (AMD) disorders [34, 36, 59–70], defects in photoreceptor function incriminating photoreceptor degeneration in diabetic retinopathy [71], glaucoma [72], and others. The fundamental biological reality is that, regardless of the initiator of the retinal insult or degeneration, if afferent activity from the photoreceptors is lost, the neural retina responds in a dynamic fashion by altering the function and connectivity of the remaining cells at the tissue, cellular, and molecular levels.

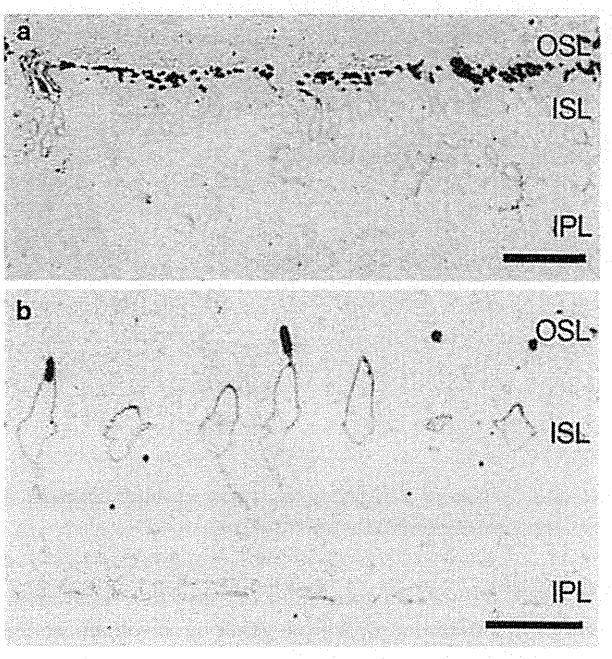

Fig. 1 Human retina from a male patient with retinitis pigmentosa. Rod opsins reveal dramatic shortening of outer segments in **a**. Rod and LWS cone opsins are shown in phase one of retinal degeneration **a** and **b**, demonstrating photoreceptor stress through opsin delocalization from where it should normally be found in the outer segments; it now extends to the inner segments and the inner plexiform layer. *Scale bar* 10 μm

Retinal remodeling

Defects that result in the loss of photoreceptor input to the neural retina initiate an event cascade that forever alters neural retinal structure as well as the pharmacologic response profiles of neurons in the retina and their connectivities. Retinal remodeling occurs in all forms of retinal degeneration, which is considered a true neural retinal deafferentation, passing through three phases of structural and functional revision. The first change is often subtle, but has severe implications for the physiology of the neural retina. During phase 1 remodeling in cone-sparing forms of retinal disease, the earliest forms of pathology are revealed by an initiation of photoreceptor stress that induces a cascade of events that culminates in molecular changes and eventual cell death. Cell stress is clinically occult and occurs prior to photoreceptor cell death, with one of the earliest histological indications revealed initially through both rod and cone opsin delocalization (Fig. 1). Rhodopsin delocalization in many cases extends from the inner segments of photoreceptors down to the cell membrane in processes that extend into the inner nuclear layer and ganglion cell layers [73]. Further, molecular alterations of bipolar cell dendritic glutamate receptor expression in phase 1 begins to alter the pharmacology of bipolar cells, shifting their functional phenotypes from ON responses to OFF responses [26, 74]. These earliest phases of retinal remodeling are likely clinically occult and occur prior to photoreceptor cell death [11].

Remodeling continues in phase 2 with photoreceptor death and phagocytic ablation of photoreceptor cell bodies. Additionally, Müller cell hypertrophy and the collapse of the distal scaffolding of the Müller cells in the absence of photoreceptor and bipolar cells form the Müller cell seal that isolates the neural retina from the RPE and choroid [7, 11, 24].

Bipolar cells are completely deafferented in phase 2: not only physiologically, through the elimination of glutamate receptors in the outer plexiform layer, but also anatomically, through the physical retraction of all bipolar cell dendrites, resulting in altered morphologies of bipolar cells (Figs. 2, 3). This results in the complete loss of glutamatergic input after the degeneration of rod photoreceptors, as shown in the rd mouse [75]. These changes in the rd/rd mouse also include the expression of aberrant ionotropic glutamate receptors (iGluR) on ON cone bipolar cells from postnatal day 15 (PND 15), poor functional activation of metabotropic glutamate receptors (mGluR) on both rod and ON cone bipolar cells throughout development, and the degenerative process and poor functional activation of

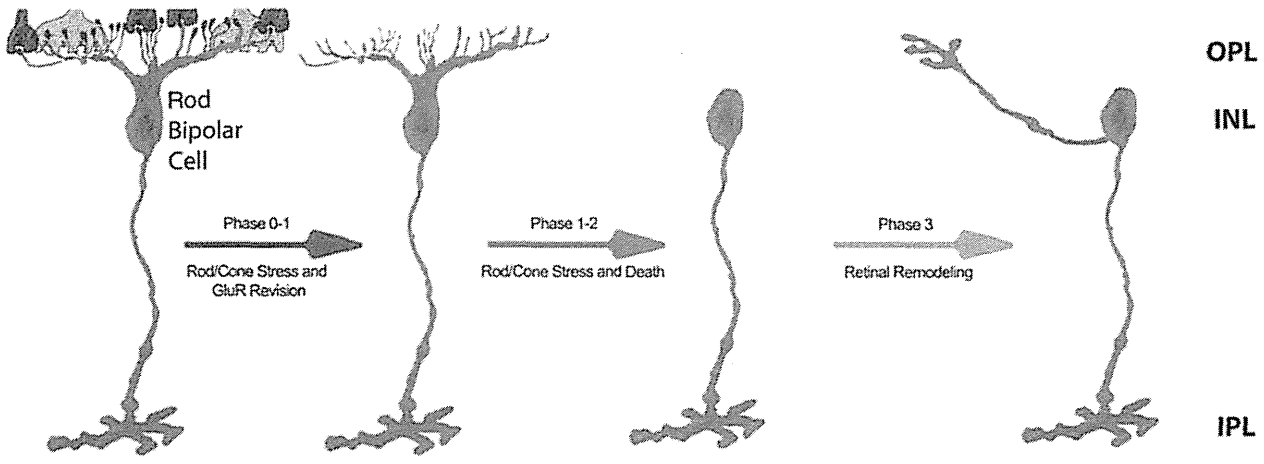

Fig. 2 In models of RP where rods and cones die simultaneously, bipolar cells lose dendrites and all iGluR/mGluR responsivity. In phase 0–1, rod bipolar cells downregulate GluR expression in the dendrites. In phase 1–2, rod and cone photoreceptor stress and death occur while dendritic modules are lost. In phase 3, wider retinal remodeling ensues, resulting in sprouting and formation of new axonal modules

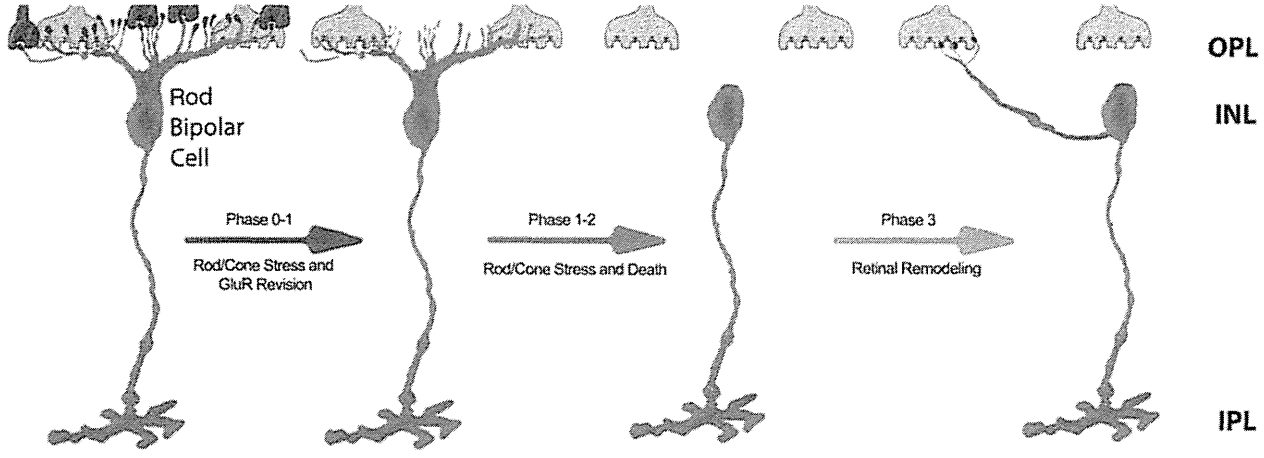

Fig. 3 In models of RP where cones outlive rods, some bipolar cell dendrites switch targets. In normal rod bipolar cell architecture, dendrites from rod bipolar cells bypass cone pedicles. In phase 0–1, as in rod/cone dystrophies, rod bipolar cells downregulate GluR expression in the dendrites. In phase 1–2 with rod stress and death, dendritic modules are lost. In late phase 2/phase 3, some rod bipolar cells form sprouts that contact cone pedicles, making peripheral contacts on cone pedicles

N-methyl-D-aspartate (NMDA) receptors on amacrine cells from PND 15 animals [76].

Retinitis pigmentosa disorders occur in both cone-sparing and cone-decimating forms. In models of RP where rods and cones die within similar time domains, retinas undergo large-scale remodeling events where bipolar cells lose dendrites and all iGluR and mGluR responsivity. Glial seal formation occurs, as does large-scale neuritogenesis leading to microneuroma formation, as well as neuronal migration [24]. In RP models where cones outlive rods (Fig. 3), some bipolar cell dendrites become involved in target switching, as shown by the fact that rod bipolar cells receive ectopic synapses from cones in the absence of rods [77], though cones may persist for some time, with Müller cells engaging in seal formation around them [24, 74]. As long as cones or remnant cone cell bodies are present, bipolar cells underneath the cone photoreceptors appear to persist and progression of the neural retina into phase 3 appears to be arrested or dramatically slowed. Other retinal changes in cone-sparing retinal degenerations in phase 2 involve the initiation of anomalous sprouting, which often coalesces into structures called microneuromas, with contributions from not only bipolar cells but also other neuronal cell classes, including amacrine cells and horizontal cells, which can be observed to extend processes down into the inner plexiform layer [20–22, 74, 78].

Phase 3 is characterized by persistent remodeling, which further revises the fundamental topology of the retina via bidirectional migration of neurons through the vertical axis of the retina, as evinced by the migration of surviving bipolar and amacrine cells into the ganglion cell layer. Conversely, in many advanced degenerate retinas in phase 3, ganglion cells can be observed migrating into the inner nuclear layer [7, 9, 11, 12, 24]. The evolution of processes from all remaining neuron types in the retina continues to occur in phase 3, with some processes forming fascicles that can run in bundles for great distances within the neural retina (>100 microns) [24], while others run together forming tangles or tufts of novel neuropils termed micro-neuromas, which form outside the normal lamination of the inner plexiform layer [7, 8, 11, 12, 24, 26, 79]. Pigmented bone spicules (Fig. 4) are a common finding in patients with RP, and are often translocated into the neural retina [80]. Pigmented bone spicules appear to co-segregate with Müller cell columns, which appear to mediate much of the gross topological restructuring and are responsible for the translocation of RPE invasion of the neural retina (Fig. 4), as well as the formation of the aforementioned pigmented bone spicules.

As phase 3 remodeling progresses, breaks in Bruch's membrane provide opportunities for some neurons to emigrate out of the neural retina proper and into the membrane choriocapillaris complex [13] (Fig. 5). Whether or not similar emigration events out of the neural retina appear in human diseases like AMD is not clear, though it seems likely in AMD and AMD-like disorders. Certainly in the late forms of AMD with vascular involvement, there are breaches of Bruch's membrane, but other evidence indicates that Bruch's membrane may become calcified following the breakdown of elastin and collagen in non-vascular or dry AMD [81].

Remodeling process variation in the presence of cones

While total loss of all photoreceptors leads to the complete loss of functional iGluR expression in ON and OFF bipolar cells, patches of cones may persist in cone-sparing forms, but they are substantially altered and embedded in the Müller cell seal. These altered cones still possess synaptic ribbons [82], but a more recent work [26] revealed that rod bipolar cells can withdraw their dendrites from rod photoreceptor terminals, subsequently elaborating transient ectopic non-ribbon contacts with surviving cone photoreceptors. Bipolar cells initiate these changes by retracting dendrites upon the loss of rod and cone contact [20–22], followed by a loss of signaling capacity in response to glutamate in regions of photoreceptor loss [75] (Figs. 2, 3). While RP disorders occur in both cone-sparing and cone-decimating forms, in cone-sparing RP, patches or isolated cones can persist for some time and appear to prolong the onset of gross topographic retinal remodeling. It is important to note that changes to network topology and iGluR/mGluR6 expression do occur in response to cone loss. Specifically, the retina underneath any remaining cone pedicles appears to be relatively preserved topologically, along with the seeming preservation of circuitry and iGluR expression in bipolar cell dendrites. However, proximal cones within 50 μm are fundamentally altered, with no iGluR signaling capacity remaining [26].

Neural information processing in the retina is immediately impacted by retinal photoreceptor degeneration and

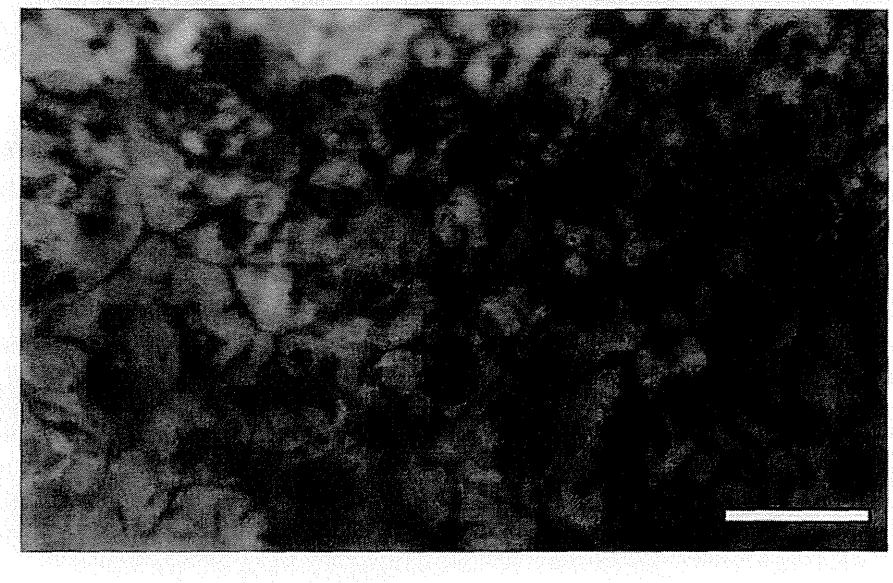

Fig. 4 Retina from a human patient with advanced RP, illustrating pigmented bone spicules—accumulations of RPE pigment granules that derive from translocations of Müller cells, which alter the topology of the neural retina and cause the accumulation of pigment along clumps, lines, and grooves in the vertical axis of the neural retina. *Scale bar* 200 μm

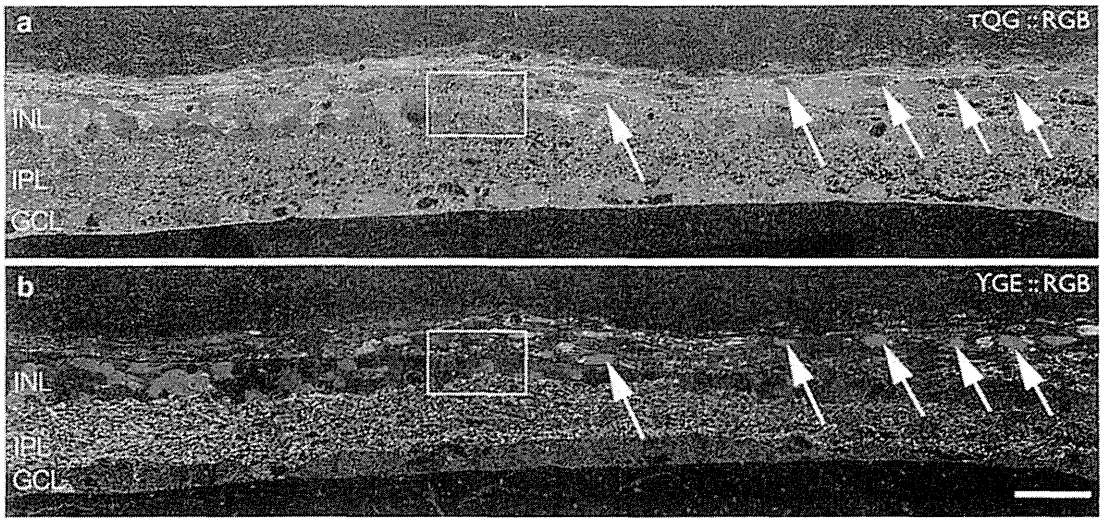

Fig. 5 Neural emigration in a light damage model of retinal degeneration in rat. Taurine, glutamine, glycine::r, g, b mapping in a demonstrates Müller glia with glycinergic amacrine cells embedded in them passing outside of the retina through a break (*box*) in Bruch's membrane. GABA, glycine, glutamate::r, g, b mapping in b demonstrates both GABAergic and glycinergic amacrine cells in addition to bipolar cells escaping from the neural retina into the choroid (*arrows*). *Scale bar* 90 μm

subsequent remodeling. The structural, biological, and information processing consequences of rod bipolar cell rewiring alone are substantial (Figs. 2, 6). The normal flow of information in the retina begins in the photoreceptors, where rod photoreceptor terminals bypass cone photoreceptor pedicles to make synapses on rod bipolar cells at their terminal spherules. Normally, hyperpolarizing signals from rod photoreceptors depolarize rod bipolar cells via sign-inverting mGluR6 receptors. Rod bipolar cells then "piggyback" onto the ON cone bipolar cell pathway through synaptic contact onto glycinergic amacrine cells that mediate signaling through to the ON cone bipolar cells via gap junctions, resulting in a sign-conserving signal, and to the OFF cone bipolar cell pathway via sign-inverting glycine receptors (Fig. 6). In cone-sparing RP, bipolar cell recordings reveal wholesale phenotype class switching from rod bipolar cells to OFF bipolar cell populations through alterations in the iGluR populations, effectively reprogramming the retina by inverting rod bipolar cell to amacrine cell to cone bipolar cell pathways, creating networks that are unable to maintain coherent signaling out of the retina [26] (Fig. 6). Additionally, from a circuit topology perspective, problems are obvious. In cone-sparing RP, the remaining cone pedicles are not numerous enough to accommodate all remaining rod bipolar cells. Furthermore, there aren't enough ribbons to accommodate rod BC dendrites, and the ON cone BCs already occupy the existing ribbon contacts. Those ectopic contacts that are formed are too far away from the ribbon to activate the existing mGluR6 receptors. Therefore, each cell type expresses receptors that are matched to concentrations that prevail at a given distance from the ribbon in normal retinas at least. If rod BC mGluR6 receptors are not activated, then rod BCs should be persistently depolarized, which presents an additional problem for visual processing.

Human diseases and animal models of retinal degeneration that show remodeling

Human tissues from patients with late-stage RP show dramatic changes to the normal architecture of the retina (Fig. 7a, b). These samples demonstrate complete loss of rod and cone photoreceptors, bipolar cell loss, and subsequent topological restructuring of the retina. YGE > rgb imaging (Fig. 7a) reveals novel tufts of neuropils, termed microneuromas [24], with amacrine cells abutting the choroid and no barrier in-between due to the absent RPE. TQE > rgb signals demonstrate the formation and elaboration of the Müller cell seal isolating the neural retina (Fig. 7b). The subretinal space in these tissues is absent and impacts potential rescue strategies. In fact, because of the adherent nature of the glial seal, experimental retinal detachments of retinas in the regions of a Müller cell seal are almost impossible without some degree of trauma to the neural retina.

One might presume that since photoreceptors are lost in retinal degenerative diseases, the neural retina would be inactive in the absence of any afferent input. However, the sprouting of the neuronal processes and the alteration of the topology of the retina beg the question of function. It turns out that, even though photoreceptors are lost in regions of

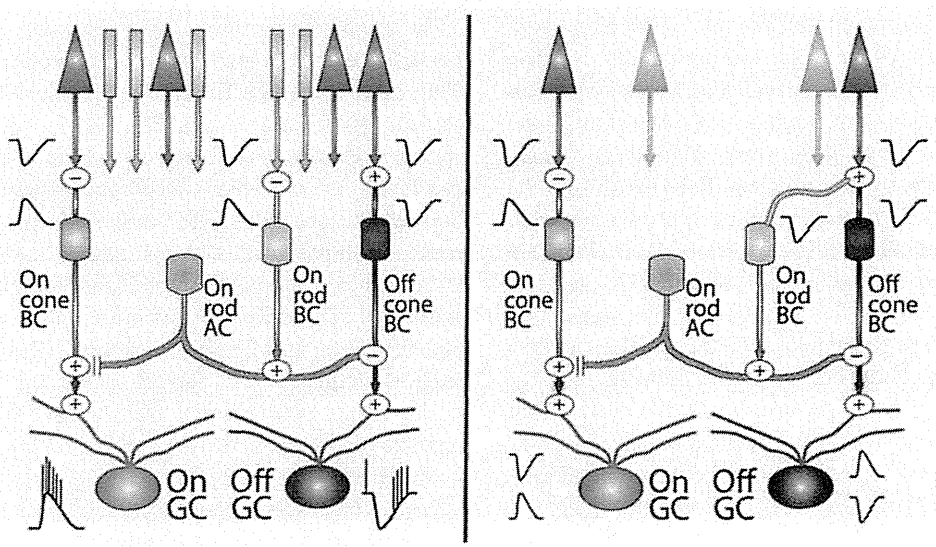

Fig. 6 Circuit diagram: rods provide sign-inverting input to ON bipolar cells via mGluR6-mediated synaptic connections. OFF bipolar cells are driven by cones through sign-conserving KA-mediated iGluRs, while ON bipolar cells are driven by cones through sign-inverting mGluR6-mediated synapses. Cone bipolar cells also synapse upon ganglion cells with sign-conserving AMPA-mediated iGluRs that define ON and OFF channels of information flow out of the retina. Information flow through the retina in humans during scotopic light levels is driven by rods and rod bipolar cells that piggyback onto intermediary amacrine cells, which shunt the flow of information to ON cone bipolar cells via sign-conserving gap junctions. Signaling to OFF cone bipolar cells occurs through sign-inverting glycinergic conventional synapses. In sum, a flash of light hyperpolarizes rod photoreceptors, and the network preserves the ON and OFF channel polarities. However, in cone-sparing RP seen in human and animal models, network flows are compromised through the formation of pathological networks that generate conflicting signaling driven by the remaining cones. With cone degeneration, this cone signaling is eventually lost, and retinas are driven by signaling intrinsic to the remnant neural retinal amacrine and ganglion cells

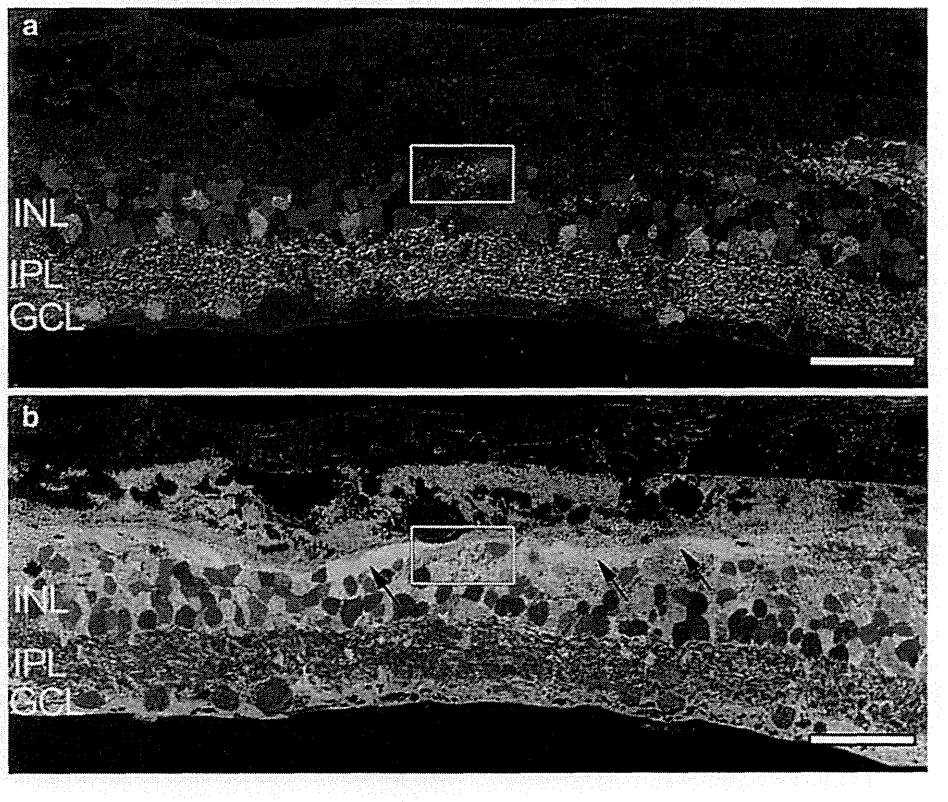

Fig. 7 Imaging of human retina from late-stage RP. GABA, glycine, glutamate::r, g, b mapping in **a** reveals novel tufts of neuropil, termed microneuromas (*box*), with amacrine cells abutting Bruch's membrane and the choroid. **b** Taurine, glutamine, glycine::r, g, b mapping of the same region demonstrates Müller cell revision and Müller cell seal formation (*arrows*), walling off the neural retina. *Scale bar* 90 μm

retinal atrophy, the neurons that are left in the retina continue to signal. Previous work examining the intrinsic activity of the *rdcl* mouse revealed dramatic levels of activity in the amacrine and ganglion cells, even though the bipolar cells were silent [26], while traditional electrophysiologic methods by Margolis and Detwiler [83] in the *rd1* mouse reveal substantial increases in oscillatory spike activity in the ganglion cells. Prior work by Pu et al. [17] in the RCS rat as well as Stasheff [19] in the *rd1* mouse and Sekirnjak et al. [84] in the P23H rat using single unit recording also shows substantial increases in the numbers of spontaneous ganglion cell spikes, despite the loss of photoreceptors to drive retinal activity. While results from single unit recording have yet to be correlated to retinas from human patients with RP, other recording methodologies were able to correlate retinal, specifically bipolar cell activity in both human and animal models of RP, which revealed identical disease mechanisms in both human and models of cone-sparing RP.

By combining excitation mapping with computational molecular phenotyping (CMP) [10], activated neurons (whether by ligands or light pathways) can be visualized ex vivo using small molecular probes. Simultaneous imaging of an activity probe, 1-amino-4-guanidobutane (AGB, functioning as a nonselective marker of ionotropic glutamatergic activity), combined with the visualization of other intrinsic small molecular signals [10], allows for the interrogation of neuronal cell classes that have been activated by either endogenous light drive or by pharmacologic activation (Fig. 8). Using CMP to segment images based upon their intrinsic small molecular signals allows the simultaneous extraction of excitation histograms revealed by AGB permeation for each class of bipolar cell, allowing the discrimination of OFF bipolar cell classes from ON bipolar cell classes. Additionally, ON bipolar cell classes can be segmented into rod and cone classes, allowing the elucidation of response profiles to AMPA [26, 74].

In remodeling retinas, amacrine and ganglion cells continue to encode signals via iGluR receptor complexes. This is an important finding, as identical findings in the mouse, rabbit, and human [26, 74] in relation to cone-sparing RPs demonstrate that after CMP segmentation, the incidence of OFF-like iGluR-expressing bipolar cells doubles in cone-sparing RP, while the incidence of remnant rod bipolar cells drops nearly tenfold. However, there appears to be no detectable bipolar cell death, leading to the conclusion that most rod bipolar cells make new contacts and begin to express iGluRs, leading to significant implications for retinal wiring. In these cases where cones outlive rods, the rod BCs actively downregulate the expression of dendritic glutamate receptor modules and retarget them to cone pedicles. The outcome is mGluR6 to iGluR phenotype switching and substantial corruption of cone pathway signaling. Conversely, in RP disorders where both rod and cones die concurrently, all BCs engage in the disassembly of iGluR modules in the dendrites, repress GluR expression, and form supernumerary axons in combination with substantial neuronal death. Mixed cone-decimating and cone-sparing zones are also possible in both human RP and animal models [26, 74].

The spectrum of diseases in humans that include retinal degeneration and subsequent remodeling is broader than widely considered. Studies show that RP and animal models of RP demonstrate and duplicate features of human retinal degeneration and remodeling. Mouse, rat, pig, dog, cat, and rabbit models of retinal degeneration are extensively documented [7–9, 11–13, 20–22, 24, 26, 74, 85–90]. Porcine P23H models of RP show a progressive loss of photoreceptors (Fig. 9a–d) with a concomitant loss of visual percepts as measured by ERG [91]. Additionally, these porcine models demonstrate aberrant Müller cell signatures (Fig. 9a) identical to those observed in human (Figs. 7b, 12b, inset), rodent, and rabbit (Fig. 10b) [74].

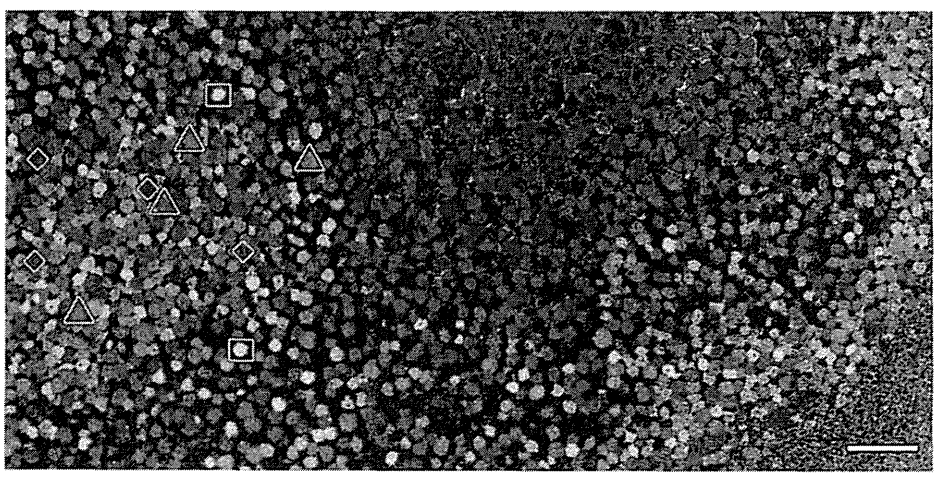

Fig. 8 Excitation recording with KA and AGB in horizontal sections through the bipolar cell layer of a 12-week old TgP347L rabbit retina visualized with glycine, AGB, glutamate::r, g, b mapping, showing that most (~82 %) of the bipolar cells have phenotypically switched from rod (*diamonds*) and ON-like BC (*squares*) responses to OFF-like BC (*triangles*) responses, revealing a fundamental molecular reprogramming of response states. *Scale bar* 60 μm